AD-A036 446 MASSACHUSETTS INST OF TECH CAMBRIDGE FLUID DYNAMICS --ETC F/G 20/8
REACTION PROBABILITIES IMPLIED BY MULTIPLE GAS-SURFACE INTERACT--ETC(U)
DEC 76 J R WILLIAMS, J R BARON F44620-75-C-0040

UNCLASSIFIED 76-1 AFOSR-TR-77-0102 NL

1 OF 1
ADA036446

END
DATE FILMED
3-77

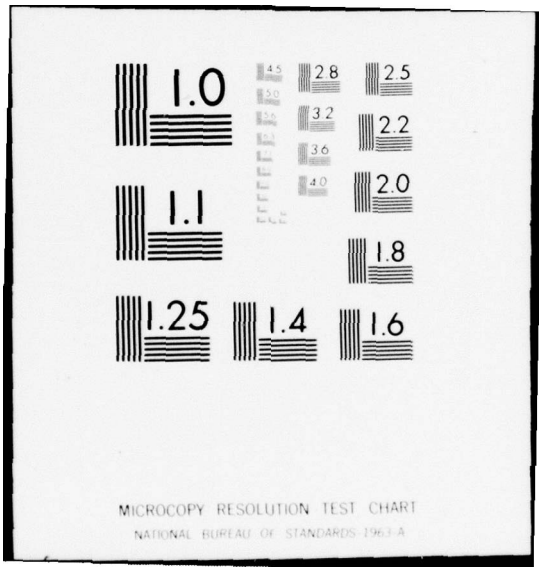
1.0
1.1
1.25
1.4
1.6
1.8
2.0
2.2
2.5
2.8
3.2
3.6
4.0
4.5
5.0
MICROCOPY RESOLUTION TEST CHART
NATIONAL BUREAU OF STANDARDS 1963-A

MASSACHUSETTS INSTITUTE OF TECHNOLOGY

Department of Aeronautics and Astronautics

Fluid Dynamics Research Laboratory

Technical Report 76-1

REACTION PROBABILITIES IMPLIED BY MULTIPLE GAS-SURFACE INTERACTIONS

J. R. Williams and J. R. Baron

December 1976

Air Force Office of Scientific Research

Contract No. F44620-75-C-0040

MIT OSP 82450

FORWARD

This investigation was sponsored by the United States Air Force Office of Scientific Research under Contract No. F44620-75-C-0040. Mr. Paul A. Thurston served as Project Manager.

ABSTRACT

The probabilities of single and two successive gas surface collisions satisfying minimum interaction energy cutoffs are considered in the hard cube model sense. Comparison is made with atomic and molecular oxygen reaction probabilities with graphite corresponding to specific mass ratio examples of 4/3 and 8/3. Comparable peak probabilities result for multiple interactions but of much reduced sharpness with temperature for only a two collision constraint. Realistic activation energies are implied from a match of the energy cutoff probability model to the portion of the experimental data increasing with surface temperature. The rapidly decreasing reaction probabilities found experimentally at higher temperatures imply an appreciable increase in the required number of effective collisions.

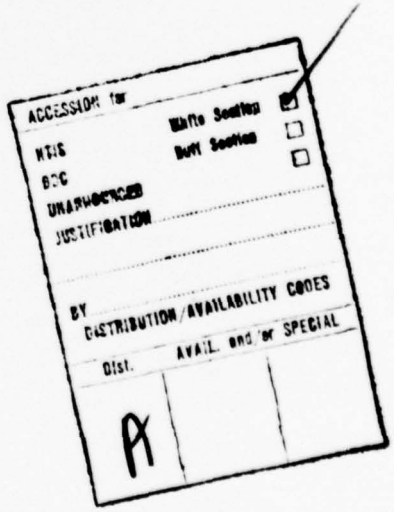

TABLE OF CONTENTS

TABLE OF CONTENTS, cont.

SYMBOLS

A, B_i	regions of (u_o, v_o) plane used for P_{II} evaluations
A, B, C, D	integration limit parameters for I_j, Equations (40), (41)
G	distribution function for surface particle speed $\|v_o\|$, Equation (1)
H	distribution function for gas particle normal velocity component u_o, Equation (2)
I_j $(\bar{u}_o)$	integral form, Equations (40), (42)
J_j $(\bar{u}_o)$	integral form, Equation (43)
K_j	Equations (45), (48)
k	Boltzman constant
k_i	slope of border to B_i region
L_j	Equation (58)
L	surface "box" length; also integration limit for J_j
M_j	Equations (50), (51)
m_g	gas particle mass
m_s	surface particle mass
m*	reduced mass, $m_s\, m_g\, /(m_s + m_g)$
N	Equation (49)
$dP_{loc\ x}$	surface particle location probability, Equation (20)
P_D	directional probability that first collision is inward or outward for given (u_o, v_o) pair, Equation (25)
P_2	probability that second collision follows from (u_o, v_o) first collision
$P_I(\bar{\epsilon})$	probability of first collision with interaction energy in excess of $\bar{\epsilon}_1$
$P_{II}(\bar{\epsilon}_1, \bar{\epsilon}_2)$	probability of second collision with interaction energy in excess of $\bar{\epsilon}_1$, $\bar{\epsilon}_2$ for first, second collisions respectively

P_i, Q_i, R_i	coefficients in integrand of B_i region contribution to P_{II}, Equation (65)
T_g	incident gas temperature
T_s	surface temperature
$\bar{T}$	$T_s/T_g \cos^2\theta$, Equation (41)
T^*	$(\mu\bar{T})^{-1/2}$
U	integration limit for J_j
u_o	gas particle normal velocity component prior to first collision, positive inward
u_1	gas particle normal velocity component after first collision, positive inward
$\bar{u}_o$, $\bar{v}_o$	normalized particle velocities, $x_g^{1/2}u_o$, $x_s^{1/2}v_o$
v_o	surface particle velocity prior to both first collision and/or rebound, positive outward
$v_{o\ coll}$	surface particle velocity immediately prior to first collision, positive outward
v_{oi}	v_o on cut-off energy, ε_i, locus, Equations (8), (17)
v_1	surface particle velocity after first encounter, positive inward
x	distance from outer edge of surface, positive inward
x*	first collision location
$(x^*/L)_m$	minimum location (normalized) for first collision which allows second collision possibility, Equation (27)
x_g	$m_g/2kT_g\cos^2\theta$
x_s	$m_s/2kT_s$
y	Equation (52)
ε_i	Cut-off energy for first collision
$\bar{\varepsilon}_i$	nondimensional cut-off energy, Equation (11)

$\bar{\varepsilon}_I$, $\bar{\varepsilon}_{II}$	first, second collision relative integration energy, Equations (7), (12)
$(\varepsilon_R)_j$	reaction probability for oxygen on graphite, j = 0, 0_2, Equation (72)
ε^*	$[(1 + \mu)\bar{\varepsilon}_1]^{1/2}$
θ	incidence angle measured from surface normal
μ	ratio of gas to surface particle masses, m_g/m_s

CHAPTER 1

INTRODUCTION

Measured reaction probabilities for both molecular and atomic oxygen reactions with carbon show anomalous (peaked) Arrhenius plots.[1,2,3,4] Comparison of results for the molecular and atomic oxidation cases indicate the atom reactivity to be higher by an order of magnitude.[1,4] It has been suggested that the increase may be related to a higher sticking probability,[1] and that dissociative adsorption may be the limiting step in the reaction mechanism.[2,4]

There is some evidence that primarily normal energy barriers are important in the dissociative adsorption and/or recombinative desorption processes.[5-9] In simplest form, interactions with greater (normal) energies than some cut-off energy will then lead to adsorption in dissociated form. For a gas at rest with respect to an adjacent solid surface the intensity of all particles impinging on the surface varies as the cosine of the angle from the surface normal. However, the intensity is non-cosine for those particles with normal energies greater than some non-zero cut-off, and the distribution is then peaked in the normal direction.

Measured distributions for the desorbing CO product of the reaction in fact vary as $\cos^2\theta$ [3,4] and imply possible normal energy barriers for the recombinative desorption process as well. It has been argued that dissociation adsorption and recombinative desorption are reverse processes[5,6] which suggests normal energy barriers for dissociative adsorption of CO.

These observations add to the importance of the normal interaction, which if dominant offers considerable simplification in modeling the events of gas and solid particle encounters. The hard-cube model[10] has had some success with precisely that assumption assuming surface particles confined to a rigid box and interacting with the normal component of Maxwellian gas particles. However, a single collision restriction was imposed by limiting the mass ratio of gas and surface particles to be $\mu < 1/3$. Primary interest at the time was in inert gas scattering distributions, for which there was comparison data from experiment and with which there proved to be quite reasonable agreement.

For reaction encounters the natural extension of a hard-cube approach is an allowance for an energy barrier and removal of the $\mu < 1/3$ constraint. The former corresponds to imposing a reaction probability, while the latter introduces multiple collisions which may weight the probability according to changes in the residence time on the surface. Single and double collision interactions are considered here while retaining the simplifying assumption of negligible lateral interaction. Thus, near normal encounters are implied and with only one atom of the solid surface.

CHAPTER 2

COLLISION PROBABILITIES MODEL

2.1 Distribution Function Basis for Probability

Goodman[11] points out that for $\mu = m_g/m_s < 1/3$ certain types of two successive collision sequences are ruled out, and that for $\mu < 1$ there will be two collisions at most. However, an oxygen-graphite encounter corresponds to $\mu > 1$, (i.e., either 16/12 or 32/12) and multiple collisions must be expected here.

We assume a constant speed surface particle moving normal to the surface and instantly reversing direction at the ends of its one dimensional box enclosure.[10,11] Immediately prior to a first collision its velocity is $v_{o\ coll}$, positive in the outward direction, and of magnitude $0 \leq |v_{o\ coll}| \leq \infty$. The probability of a first collision involving $|v_{o\ coll}|$ $(=|v_o|)$ is the probability that the speed is $|v_o|$ at the time the gas particle enters the box. From the one dimensional Maxwellian distribution this is

$$G(|v_o|)\,dv_o = 2(\chi_s/\pi)^{1/2} \exp(-\chi_s v_o^2)\,dv_o \qquad (1)$$

where $\chi_s = m_s/2kT_s$.

An approaching gas particle in a Maxwellian beam oriented at an angle θ from the surface normal has a normal velocity component u_o, positive inward, with the distribution $(o \leq u_o \leq \infty)$:

$$H(u_o)\,du_o = 2\chi_g^2 u_o^3 \exp(-\chi_g u_o^2)\,du_o \qquad (2)$$

where $x_g = m_g / 2kT_g \cos^2\theta$.

Classical encounters will be assumed between the surface and gas particles along the normal direction. Tangential interactions are neglected and clearly this is a progressively poorer approximation with an increasing number of collisions prior to departure of the gas particle from the box. Indeed, for a sufficiently large number of collisions it should be expected that a substantial part of the tangential momentum is absorbed for any one gas particle. Should a second collision occur it is assumed to be with the same surface particle. The tangential and second collision assumptions together effectively limit the range of θ to "near" zero. The explicit ap earance of θ is then solely in x_g, and in the combination $T_g\cos^2\theta$, and is effectively then a beam cooling parameter.

Consider the probability that a first collision occurs for a specific interaction energy. For such collisions to occur prior to rebound of the surfact particle

$$\text{either, } v_{o_{coll}} = v_o > 0 \quad \text{, for an outward type}$$

$$\text{or, } v_{o_{coll}} = v_o < 0 \quad \text{, for an inward type} \qquad (3)$$

whereas if rebound precedes the collision,

$$v_{o_{coll}} = -v_o > 0 \quad \text{, for an outward type} \qquad (4)$$

This may be interpreted as an increased directional probability, $P_D(u_o, v_o)$, for the $v_o > 0$, i.e., outward type, collisions and a corresponding decrease in the probability for $v_o < 0$, i.e., inward type, collisions. With that understanding, the probability of a first collision with $v_{o\ coll} = v_o$ is

$$dP_I = P_D(u_o, v_o)\, H(u_o)\, G(|v_o|)\, dv_o\, du_o \qquad (5)$$

at a point in the (u_o, v_o) half plane. Only some fraction of these will result in a second collision. If $P_2(u_o, v_o)$ is the probability of a second collision resulting from an initial (u_o, v_o) pair for the first collision, then

$$dP_{II} = P_2(u_o, v_o)\, dP_I \qquad (6)$$

is the overall second collision probability for a point in the (u_o, v_o) half plane. Integration of Equations (5) and (6) over portions of the half plane ($0 \le u_o \le \infty$; $-\infty \le v_o \le \infty$) furnishes the proportional number of first and second collisions relative to the number of gas particles arriving at the surface.

In view of the P_D weighting in Equation (5) only Equation (3) (i.e. $v_{o\ coll} = v_o$) need be considered and the relative interaction energy for a first collision is [12]

$$\epsilon_I = \frac{m^*}{2}(u_o + v_o)^2 \qquad (7)$$

in terms of a reduced mass are* $= m_s m_g/(m_s + m_g)$. Here $v_o \ge -u_o$ since <u>all</u> lesser speeds correspond to Equation (4). For relative energies equal or greater than a cut-off energy ϵ_1, say, Equation (7) imposes the constraint (Fig. 1):

$$v_o \ge \sqrt{\frac{2\epsilon_1}{m^*}} - u_o \quad (= v_{o1}, \text{ say}) \qquad (8)$$

The relative number of such collisions is, then, from Equation (5),

$$P_I(\epsilon_1) = \int_0^\infty \int_{v_{0_1}}^\infty P_D H G(|v_0|)\, dv_0\, du_0 \tag{9}$$

It is worth noting the limiting case of $T_s \to 0$ for which $|v_0| \to 0$ and $u_0 \geq \sqrt{2\epsilon_1/\mu^*}$; i.e.,

$$P_I(\bar{\epsilon}_1)_{T_2 \to 0} = \int_{\sqrt{2\epsilon_1/\mu^*}}^\infty H\, du_0 = \left[1 + (1+\mu)\bar{\epsilon}_1\right] e^{-(1+\mu)\bar{\epsilon}_1} \tag{10}$$

in which

$$\bar{\epsilon}_i = \frac{\epsilon_i}{k T_2 \cos^2\theta} \tag{11}$$

is the natural nondimensional interaction cut-off energy.

A second collision energy cut-off follows from the relative interaction energy

$$\epsilon_{II} = \frac{\mu^*}{2}(u_1 + v_1)^2 \qquad [u_1 > -v_1] \tag{12}$$

where u_1, v_1 are the particle speeds immediately after the first encounter. The sign choice in Equation (12) follows from $v_1 > 0$ for $\mu > 1$ since from momentum and energy considerations

$$u_1 = \frac{(\mu-1)u_0 - 2v_0}{\mu+1}$$

$$v_1 = \frac{2\mu u_0 + (\mu-1)v_0}{\mu+1} \tag{13}$$

if a collision occurs ($v_0 \geq -u_0$). Here both u_1, v_1 are positive inward. As a consequence, the second collision occurs, if at all, after the surface particle rebounds from the bottom of the box, and the relative speed is then $(u_1 + v_1)$ for $u_1 \gtrless 0$. From Equation (13) a second collision always (i.e., $P_2 = 1.0$) takes place for

$$v_0 \leq \frac{\mu-1}{2} u_0 \quad , \quad \text{i.e. } u_1 \geq 0 \, , \tag{14}$$

and takes place for

$$v_0 > \frac{\mu-1}{2} u_0 \quad , \quad \text{i.e. } u_1 < 0 \, , \tag{15}$$

only if the gas particle is overtaken prior to its departure from the surface (i.e. $P_2 < 1.0$).

A cut-off constraint for interaction energies $\geq \epsilon_2$ is then

$$v_1 \geq \sqrt{\frac{2\epsilon_2}{m^*}} - u_1 \tag{16}$$

and corresponds to (Fig. 1):

$$v_0 \lesssim \frac{1}{3-\mu} \left[(3\mu-1) u_0 - (\mu+1) \sqrt{\frac{2\epsilon_2}{m^*}} \right] \quad (= v_{0_2}, \text{say}) \tag{17}$$

for $\mu \lesssim 3$ on introducing Equation (13). The $T_s \to 0$ limit here implies

$$u_0 > \frac{\mu+1}{3\mu-1} \sqrt{\frac{2\epsilon_2}{m^*}} \tag{18}$$

for both $\mu \lesssim 3$. Since $P_2 = 1$ for $|v_0| \to 0$ in view of Equation (14),

$$P_{II}(\bar{\epsilon}_1, \bar{\epsilon}_2)_{\bar{\epsilon}_2 \to 0} = \int_{\mu_i\sqrt{\frac{2\bar{\epsilon}_i}{\mu+1}}}^{\infty} H\,du_o = \left[1 + (1+\mu)\mu_i^2\bar{\epsilon}_i\right] e^{-(1+\mu)\mu_i^2\bar{\epsilon}_i} \tag{19}$$

where $\mu_1 = 1$, $\mu_2 = \frac{\mu + 1}{3\mu - 1}$, and Equation (19) requires a lower limit of integration choice which is the larger of the u_o minimums [either Equation (18) or that above Equation (10)].

2.2 Directional Probability, P_D

At the time that a gas particle enters the surface box the solid particle has neither preferred direction nor location. Thus the probability that the initial motion is either outward ($v_o > 0$) or inward ($v_o < 0$) is 1/2, and the initial location within a box of length L is

$$dP_{loc\,x} = \frac{|dx|}{L} \tag{20}$$

However, our interest is in the directional probability at the time of first impact, P_D, such that the collision itself is of an outward ($v_{o\ coll} > 0$) or inward ($v_{o\ coll} < 0$) type for a given (u_o, v_o) pair. Clearly all $v_o > 0$ will result in outward collisions. In addition some $v_o < 0$ [see Equation (4)] also lead to outward collisions if rebound occurs prior to being overtaken by the gas particle. It follows that inward collisions will occur for only the remaining $v_o < 0$ particles.

If $-u_o < v_o < 0$ the times required for the surface and gas particles to reach the bottomeof the box are $(L - x)/|v_o|$ and L/u_o respectively. The initial locations

$$\frac{x}{L} \leq 1 - \frac{|v_0|}{u_0} \tag{21}$$

therefore imply overtaking (inward, $v_{o\ coll} < 0$) and rebound (outward, $v_{o\ coll} > 0$) collisions respectively when $v_o < 0$. Combining the initial direction probabilities with Equation (20) for the box regions of Equation (21):

$$P_{D_{INWARD}} \atop (v_{o_{COLL}}<0) = \begin{cases} 0 & (\ v_0 < -u_0\ ) \\ \left(\int_0^{L(1-\frac{|v_0|}{u_0})} \frac{dx}{L}\right)\left(\frac{1}{2}\right) = \frac{1}{2}\left(1-\frac{|v_0|}{u_0}\right) & (-u_0 < v_0 < 0) \\ 0 & (\ 0 < v_0\ ) \end{cases} \tag{22}$$

OVERTAKING DIRECT

$$P_{D_{OUTWARD}} \atop (v_{o_{COLL}}>0) = \begin{cases} 1/2 & (\ v_0 < -u_0\ )_{REBOUND} \\ \left(\int_{L(1-\frac{|v_0|}{u_0})}^{L} \frac{dx}{L}\right)\left(\frac{1}{2}\right) = \frac{|v_0|}{2u_0} & (-u_0 < v_0 < 0)_{REBOUND} \\ 1/2 & (\ 0 < v_0\ )_{HEAD\ ON\ DIRECT} \end{cases} \tag{23}$$

for any v_o the probability of a first collision is $P_{Din} + P_{Dout}$ so that

$$P_I = \int_0^{\infty} H\left\{\int_{-\infty}^{-u_0}\left(0+\frac{1}{2}\right)+\int_{-u_0}^{0}\frac{1}{2}\left(1-\frac{|v_0|}{u_0}\right)+\frac{|v_0|}{2u_0}+\int_0^{u_0}\left(0+\frac{1}{2}\right)+\int_{u_0}^{\infty}\left(0+\frac{1}{2}\right)\right\} G(|v_0|)\,dv_0\,du_0 \tag{24}$$

and indicates P_I to be unity for the entire half plane as would be expected.

With energy constraints such as Equation (8) it is more convenient to collect the inward and outward contributions together to obtain the equivalent directional probability as in Equation (5). I.e.,

$$P_b(u_0, v_0) = \begin{cases} P_{out}_{v_0>0} + P_{out}_{v_0<0} = \left\{ \begin{array}{ll} 1 & (u_0 < v_0) \\ \frac{1}{2}\left(1+\frac{|v_0|}{u_0}\right) & (0 < v_0 < u_0) \end{array} \right\} = \frac{1}{2}\left(1+\frac{v_0}{u_0}\right) \\ P_{in}_{v_0<0} = \left\{ \begin{array}{ll} \frac{1}{2}\left(1-\frac{|v_0|}{u_0}\right) & (-u_0 < v_0 < 0) \\ 0 & (v_0 < -u_0) \end{array} \right. \end{cases} \quad (25)$$

to indicate outward type collisions ($v_{0\ coll} > 0$) are more probable for a given $|v_0|$, and that the overall probability for any $|v_0|$ is in fact unity for a first collision (Figure 2). E.g., for the entire half plane Equation (24) may then be written as

$$P_I = \int_0^\infty H \left\{ \int_{-u_0}^{0} \frac{1}{2}\left(1-\frac{|v_0|}{u_0}\right) + \int_0^{u_0} \frac{1}{2}\left(1+\frac{|v_0|}{u_0}\right) + \int_{u_0}^{\infty} \right\} G(|v_0|)\, dv_0 du_0 \quad (25a)$$

2.3 Second Collision Probability, P_2

A second collision is certain if $v_{0\ coll} \leq (\mu - 1)/2u_0$ in view of Equation (14). Thus

$$P_2(u_0, v_{0\ coll}) = 1 \qquad \left[v_{0\ coll} \leq \frac{\mu-1}{2} u_0 \right] \quad (26)$$

The remaining portion of the (u_0, v_0) half plane involves only outward $v_0 > 0$ first collisions with $u_1 < 0$ as in Equation (15). Some of these collisions take place at a location, x^* say, which permits the surface particle to then rebound from the bottom of its box and overtake the gas particle for a second collision. P_2 follows from the probability that

a first collision will occur within the allowable x* range consistent with the arbitrary surface particle location, Equation (20), and direction initially.

Allowable x* locations are those for which the gas particle exit time, $x^*/(-u_1)$, exceeds the equivalent time for the surface particle, $(2L - x^*)/v_1$. Using Equation (13), overtaking second collisions correspond to first collisions in the range

$$1 \geq \frac{x^*}{L} \geq \frac{2\left(2\,\frac{v_{o\,coll}}{u_o} - (\mu - 1)\right)}{(\mu+1)\left(1 + \frac{v_{o\,coll}}{u_o}\right)} \quad \left[= \left(\frac{x^*}{L}\right)_{lm},\ say\right] \tag{27}$$

Larger $(v_{o\ coll}/u_o)$ imply a smaller range of allowable locations. For $(v_{o\ coll}/u_o) = (\mu - 1)/2$ the collision may occur anywhere in the box, consistent with Equation (26). For $\mu > 3$ there is an allowable range for all $(v_{o\ coll}/u_o) < \infty$; for $\mu < 3$ a sufficiently large $v_{o\ coll}/u_o$ $[> (3\mu - 1)/(3 - \mu)]$ cannot result in an overtaking second collision, consistent with the energy constraint in Equation (17) when $\varepsilon_2 = 0$.

Since outward $(v_{o\ coll} > 0)$ first collisions arise from both $v_o \lesseqgtr 0$ the collision site differs for each initial direction. Equating the times for the two particles, the first collision occurs at

$$\frac{x^*}{u_o} = \begin{cases} \dfrac{x - x^*}{v_o} & (v_{o\,coll} = v_o > 0) \\ \dfrac{L - x}{|v_o|} + \dfrac{L - x^*}{|v_o|} & (v_{o\,coll} = -v_o > 0) \end{cases} \tag{28}$$

or

$$\frac{x^*}{L} = \begin{cases} \left(\frac{x}{L}\right)\left(1+\frac{v_0}{u_0}\right)^{-1} & \left(v_{0_{coll}} = v_0 > 0\right) \\ \left(2-\frac{x}{L}\right)\left(1+\frac{v_0}{u_0}\right)^{-1} & \left(v_{0_{coll}} = -v_0 > 0\right) \end{cases} \tag{29}$$

The probability that the collision occurs within d(x*/L) is then

$$dP_{loc\,x^*} = \frac{1}{2}\frac{|dx|}{L} = \frac{1}{2}\left(1+\frac{|v_0|}{u_0}\right)\frac{|dx^*|}{L} \qquad (v_0 \leq 0) \tag{30}$$

and the collisions are in the ranges, from Equation (29),

$$0 \leq \frac{x^*}{L} \leq \left(1+\frac{v_0}{u_0}\right)^{-1} \qquad \left(0 \leq \frac{x}{L} \leq 1\right)$$

$$\left(1+\frac{|v_0|}{u_0}\right)^{-1} \leq \frac{x^*}{L} \leq \begin{cases} 1 & \left(1 \geq \frac{x}{L} \geq 1-\frac{|v_0|}{u_0}\right) \\ 2\left(1+\frac{|v_0|}{u_0}\right)^{-1} & \left(1 \geqslant \frac{x}{L} \geqslant 0\right) \end{cases} \tag{31}$$

The limitation on initial locations x/L for the inward directed surface particles with velocities between $0 > v_0/u_0 > -1$ corresponds to those particles that rebound and thereafter undergo an outward ($v_{0\ coll} > 0$) interaction (Equation 21). Note that there is an implicit influence of the mass ratio, μ, in Equation (31) by virtue of the present interest in $(v_{0\ coll}/u_0) > (\mu - 1)/2$.

The second collision probability, P_2, follows from Equation (30) applied to those portions of the first collision ranges, Equation (31), which fall within the allowable range for a second collision, Equation (27).

For the direct outward ($v_0 > 0$) interactions: $[(\mu - 1)/2 < v_0/u_0]$

If $\left(\frac{x^*}{L}\right)_m < \left(1+\frac{v_0}{u_0}\right)^{-1}$, i.e. $\frac{\mu-1}{2} < \frac{v_0}{u_0} < \frac{3\mu-1}{4}$

$$P_2 = \int_{(x^*/L)_m}^{(1+\frac{v_0}{u_0})^{-1}} \frac{1}{2}\left(1+\frac{v_0}{u_0}\right) d\left(\frac{x^*}{L}\right) = \frac{3\mu-1-4\frac{v_0}{u_0}}{2(\mu+1)} \tag{32a}$$

If $\left(\frac{x^*}{L}\right)_m > \left(1+\frac{v_0}{u_0}\right)^{-1}$, i.e. $\frac{3\mu-1}{4} < \frac{v_0}{u_0}$

$$P_2 = 0 \tag{32b}$$

For the rebound outward ($v_0 < 0$) interactions; for $(\mu - 1)/2 < 1 < |v_0|/u_0$:

If $\left(\frac{x^*}{L}\right)_m < \left(1+\frac{v_0}{u_0}\right)^{-1}$, i.e. $\frac{\mu-1}{2} < \frac{|v_0|}{u_0} < \frac{3\mu-1}{4}$

$$P_2 = \int_{(1+\frac{v_0}{u_0})^{-1}}^{2(1+\frac{v_0}{u_0})^{-1}} \frac{1}{2}\left(1+\frac{|v_0|}{u_0}\right) d\left(\frac{x^*}{L}\right) = \frac{1}{2} \tag{33a}$$

If $\left(1+\frac{|v_0|}{u_0}\right)^{-1} < \left(\frac{x^*}{L}\right)_m < 2\left(1+\frac{|v_0|}{u_0}\right)^{-1}$, i.e. $\frac{3\mu-1}{4} < \frac{|v_0|}{u_0} < \mu$

$$P_2 = \int_{(x^*/L)_m}^{2(1+\frac{|v_0|}{u_0})^{-1}} \frac{1}{2}\left(1+\frac{|v_0|}{u_0}\right) d\left(\frac{x^*}{L}\right) = 2\left(\frac{\mu-\frac{|v_0|}{u_0}}{\mu+1}\right) \tag{33b}$$

If $2\left(1+\frac{|v_0|}{u_0}\right)^{-1} < \left(\frac{x^*}{L}\right)_m$, i.e. $\mu < \frac{|v_0|}{u_0}$

$$P_2 = 0 \tag{33c}$$

and for $(\mu - 1)/2 < |v_o|/u_o < 1$:

If $\left(\frac{x^*}{L}\right)_m < \left(1 + \frac{|v_o|}{u_o}\right)^{-1}$, i.e. $\frac{\mu-1}{2} < \frac{|v_o|}{u_o} < \frac{3\mu-1}{4}$

$$P_2 = \int_{\left(1+\frac{|v_o|}{u_o}\right)^{-1}}^{1} \frac{1}{2}\left(1 + \frac{|v_o|}{u_o}\right) d\left(\frac{x^*}{L}\right) = \frac{1}{2}\frac{|v_o|}{u_o} \tag{34a}$$

If $\left(1+\frac{|v_o|}{u_o}\right)^{-1} < \left(\frac{x^*}{L}\right)_m$, i.e. $\frac{3\mu-1}{4} < \frac{|v_o|}{u_o} < 1$

$$P_2 = \int_{\left(\frac{x^*}{L}\right)_m}^{1} \frac{1}{2}\left(1 + \frac{|v_o|}{u_o}\right) d\left(\frac{x^*}{L}\right) = \frac{3\mu - 1 - (3-\mu)\frac{|v_o|}{u_o}}{2(\mu+1)} \tag{34b}$$

2.4 Overall Second Collision Probability, P_{II}

The mass ratio μ provides the basis for specific integration intervals when evaluating P_{II} from Equation (6) with (25). Note that

$$\frac{3\mu-1}{3-\mu} > \mu > \frac{3\mu-1}{4} > \frac{\mu-1}{2}, \quad \text{if } \mu > 1 \tag{35}$$

and

$$\begin{aligned} \frac{3\mu-1}{4} &\gtrless 1 \quad \text{if} \quad \mu \gtrless \frac{5}{3} \\ \frac{\mu-1}{2} &\gtrless 1 \quad \text{if} \quad \mu \gtrless 3 \end{aligned} \tag{36}$$

Then for $1 < \mu < 5/3$, $5/3 < \mu < 3$, and $3 < \mu$ respectively:

$$P_{II} = \left\{ \int_0^{\infty} H \left\{ \int_{-\infty}^{-u_0} + \int_{-u_0}^{0} + \int_{0}^{\frac{\mu-1}{2}u_0} + \int_{\frac{\mu-1}{2}u_0}^{\frac{3\mu-1}{4}u_0} + \int_{\frac{3\mu-1}{4}u_0}^{u_0} + \int_{-u_0}^{\mu u_0} + \int_{\mu u_0}^{\infty} \right\} \right. \tag{37a}$$

$$\left. \int_0^{\infty} H \left\{ \int_{-\infty}^{-u_0} + \int_{-u_0}^{0} + \int_{0}^{\frac{\mu-1}{2}u_0} + \int_{\frac{\mu-1}{2}u_0}^{u_0} + \int_{u_0}^{\frac{3\mu-1}{4}u_0} + \int_{\frac{3\mu-1}{4}u_0}^{\mu u_0} + \int_{\mu u_0}^{\infty} \right\} \right. \tag{37b}$$

$$\left. \int_0^{\infty} H \left\{ \int_{-\infty}^{-u_0} + \int_{-u_0}^{0} + \int_{0}^{u_0} + \int_{u_0}^{\frac{\mu-1}{2}u_0} + \int_{\frac{\mu-1}{2}u_0}^{\frac{3\mu-1}{4}u_0} + \int_{\frac{3\mu-1}{4}u_0}^{\mu u_0} + \int_{\mu u_0}^{\infty} \right\} \right\} P_2 P_D \sigma \, dv_0 \, du_0 \tag{37c}$$

prior to any energy cut-off considerations. The essential point is the association of a proper P_2 with each P_D term in accord with the latter's direct or rebound first collision origin.

For the specific interaction of atomic oxygen and carbon, i.e., $\mu = 16/12$, the contributions from Equations (25), (26) and (32) - (34) into (37) gives (for $\varepsilon_1 = \varepsilon_2 = 0$):

$$P_{II} = \int_0^{\infty} H \left\{ \int_{-u_0}^{u_0/6} \frac{1}{2}\left(1 + \frac{v_0}{u_0}\right) + \int_{u_0/6}^{3u_0/4} \frac{7\left(\frac{v_0}{u_0}\right)^2 - 12\frac{v_0}{u_0} + 9}{28} \right.$$
$$\left. + \int_{3u_0/4}^{u_0} \frac{v_0}{u_0}\left(\frac{9 - 5\frac{v_0}{u_0}}{28}\right) + \int_{u_0}^{4u_0/3} \frac{4 - 3\frac{v_0}{u_0}}{7} \right\} \sigma \, dv_0 \, du_0 \tag{38}$$

Similarly for molecular oxygen, $\mu = 32/12$:

$$P_{II} = \int_0^{\infty} H \left\{ \int_{-u_0}^{\frac{5u_0}{6}} \frac{1}{2}\left(1 + \frac{v_0}{u_0}\right) + \int_{\frac{5u_0}{6}}^{u_0} \frac{11\left(\frac{v_0}{u_0}\right)^2 - 12\frac{v_0}{u_0} + 21}{44} + \int_{u_0}^{8u_0/3} \frac{8 - 3\frac{v_0}{u_0}}{11} \right\} \sigma \, dv_0 \, du_0 \tag{39}$$

E.g., for $\mu = 4/3$ the v_o integrals follow from

$$\int_{-\infty}^{-u_o} (1)(0) + \left(\int_{-u_o}^{0} + \int_{0}^{\frac{\mu-1}{2}u_o}\right)(1)\left(\frac{1}{2}\left[1+\frac{v_o}{u_o}\right]\right) + \int_{\frac{\mu-1}{2}u_o}^{\frac{3\mu-1}{4}u_o} \frac{3\mu-1-4\frac{v_o}{u_o}}{2(\mu+1)}\left(\frac{1}{2}\right) + \left(\frac{1}{2}\frac{v_o}{u_o}\right)^2$$

$$+ \int_{\frac{3\mu-1}{4}u_o}^{u_o} (0)\left(\frac{1}{2}\right) + \frac{3\mu-1+(3-\mu)\frac{v_o}{u_o}}{2(\mu+1)}\left(\frac{1}{2}\frac{v_o}{u_o}\right) + \int_{u_o}^{\mu u_o} (0)\left(\frac{1}{2}\right) + \left(2\frac{\mu-\frac{v_o}{u_o}}{\mu+1}\right)\left(\frac{1}{2}\right) + \int_{\mu u_o}^{\infty} (0)\left(\frac{1}{2}\right) + (0)\left(\frac{1}{2}\right)$$

where for each interval for which $v_o > u_o(\mu - 1)/2$ the explicit $[(P_2\ P_D)_{direct} + (P_2\ P_D)_{rebound}]$ terms are indicated.

The energy constraints $v_o \geq v_{o_1}$ and $v_o < v_{o_2}$ affect only the integration limits as in Figure 1. Explicit integral results are developed in the next section in appropriate nondimensional form.

CHAPTER 3

INTEGRAL FORMS

3.1. General Form

An evaluation of P_I and P_{II} involves solely the integral form

$$I_j(u_0)_{A,B}^{C,D} = \int_{Au_0+B}^{Cu_0+D} \left(\frac{v_0}{u_0}\right)^j HG\, dv_0\, du_0 \qquad [j=0,1,2] \tag{40}$$

Introducing the nondimensional parameters,

$$\bar{v}_0 = \chi_s^{1/2} v_0 \quad , \quad \bar{u}_0 = \chi_g^{1/2} u_0 \tag{41a}$$

$$\bar{B} = \chi_s^{1/2} B \quad , \quad \bar{C} = C/(\mu\bar{T})^{1/2} \tag{41b}$$

$$\bar{D} = \chi_s^{1/2} D \quad , \quad \bar{A} = A/(\mu\bar{T})^{1/2}$$

$$\mu\bar{T} = \mu \frac{T_s}{T_g \cos^2\theta} = \frac{\chi_g}{\chi_s} \tag{41c}$$

then

$$I_j(\bar{u}_0)_{\bar{A},\bar{B}}^{\bar{C},\bar{D}} = \frac{4}{\pi^{1/2}(\mu\bar{T})^{j/2}} \int \bar{u}_0^{(3-j)} e^{-\bar{u}_0^2} J_j\, d\bar{u}_0 \tag{42}$$

Here

$$J_j(\bar{u}_0) = \int_L^V \bar{v}_0^j e^{-\bar{v}_0^2} d\bar{v}_0 = \begin{cases} \frac{\pi^{1/2}}{2}(\operatorname{erf} V - \operatorname{erf} L) & [j=0] \\ \frac{1}{2}\left(e^{-L^2} - e^{-V^2}\right) & [j=1] \\ \frac{1}{2}\left(Le^{-L^2} - Ve^{-V^2} + \frac{\pi^{1/2}}{2}[\operatorname{erf} V - \operatorname{erf} L]\right) & [j=2] \end{cases} \tag{43}$$

and

$$U = \bar{C}\bar{u}_0 + \bar{D} \quad , \qquad L = \bar{A}\bar{u}_0 + \bar{B}$$

I.e.,

$$I_j(\bar{u}_0)_{\bar{A},\bar{B}}^{\bar{C},\bar{D}} = K_j(U,\bar{u}_0) - K_j(L,\bar{u}_0) \tag{44}$$

where

$$\begin{aligned} K_0(U;\bar{u}_0) &= 2\int \bar{u}_0^3 e^{-\bar{u}_0^2} \operatorname{erf} U \, d\bar{u}_0 \\ K_1(U;\bar{u}_0) &= -2\left(\frac{\mu\bar{T}}{\pi}\right)^{1/2} \int \bar{u}_0^2 e^{-\bar{u}_0^2} e^{-U^2} \, d\bar{u}_0 \\ K_2(U;\bar{u}_0) &= (\mu\bar{T}) \int \bar{u}_0 e^{-\bar{u}_0^2} \left(\operatorname{erf} U - \frac{2U}{\pi^{1/2}} e^{-U^2}\right) d\bar{u}_0 \end{aligned} \tag{45}$$

Integrating by parts, and noting that[13]

$$\int Z(\bar{u}_0) e^{-(a\bar{u}_0^2 + 2b\bar{u}_0 + c)} \, d\bar{u}_0 = \frac{\exp\left(\frac{b^2-ac}{a}\right)}{a^{1/2}} \int Z\left(\frac{y^{1/2}-b}{a}\right) e^{-y^2} dy \tag{46}$$

where

$$y = a^{1/2}\left(\bar{u}_0 + \frac{b}{a}\right) \tag{47}$$

then

$$\begin{aligned} K_0(\bar{C},\bar{D};\bar{u}_0) &= \frac{2}{\pi^{1/2}}\left[-(1+\bar{u}_0^2)N + \bar{C}(M_0 + M_2)\right] \\ K_1(\bar{C},\bar{D};\bar{u}_0) &= -\left(\frac{\mu\bar{T}}{\pi}\right)^{1/2} M_2 \\ K_2(\bar{C},\bar{D};\bar{u}_0) &= \frac{\mu\bar{T}}{\pi^{1/2}}\left[-N + \bar{C}M_0 - 2(\bar{D}M_1 + \bar{C}M_2)\right] \end{aligned} \tag{48}$$

in which

$$N(\bar{C},\bar{D},\bar{u}_0) = \frac{\pi^{1/2}}{2} e^{-\bar{u}_0^2} \operatorname{erf}(\bar{C}\bar{u}_0 + \bar{D}) \tag{49}$$

and the

$$M_i(\bar{C},\bar{D};\bar{u}_0) = \int \bar{u}_0^{\,i} e^{-[\bar{u}_0^2+(\bar{C}\bar{u}_0+\bar{D})^2]}\, d\bar{u}_0 \qquad (50)$$

are

$$M_0 = \frac{\exp\left(-\frac{\bar{D}^2}{1+\bar{C}^2}\right)}{2(1+\bar{C}^2)^{1/2}}\,\pi^{1/2}\,\mathrm{erf}\,y$$

$$M_1 = -\frac{\exp\left(-\frac{\bar{D}^2}{1+\bar{C}^2}\right)}{2(1+\bar{C}^2)}\left(e^{-y^2}+\frac{\bar{C}\bar{D}}{(1+\bar{C}^2)^{1/2}}\,\pi^{1/2}\,\mathrm{erf}\,y\right) \qquad (51)$$

$$M_2 = \frac{\exp\left(-\frac{\bar{D}^2}{1+\bar{C}^2}\right)}{4(1+\bar{C}^2)^{3/2}}\left(2\left[-y+\frac{2\bar{C}\bar{D}}{(1+\bar{C}^2)^{1/2}}\right]e^{-y^2} + \left[1+2\left(\frac{\bar{C}\bar{D}}{(1+\bar{C}^2)^{1/2}}\right)^2\right]\pi^{1/2}\,\mathrm{erf}\,y\right)$$

Here

$$y = \frac{(1+\bar{C}^2)\bar{u}_0+\bar{C}\bar{D}}{(1+\bar{C}^2)^{1/2}} \qquad (52)$$

The special limit of $|\bar{D}| \to \infty$ then corresponds to

$$\begin{aligned} M_0 &= M_1 = M_2 = K_1 = 0 \\ N &= \pm\frac{\pi^{1/2}}{2}\,e^{-\bar{u}_0^2} \\ K_0 &= \mp\,(1+\bar{u}_0^2)\,e^{-\bar{u}_0^2} \\ K_2 &= \mp\,\frac{\mu\bar{T}}{2}\,e^{-\bar{u}_0^2} \end{aligned} \qquad (53)$$

and application to Equation (24) yields

$$P_I = \int_0^{\infty}\int_{-\infty}^{\infty} \frac{HG}{2}\, d\bar{v}_0\, d\bar{u}_0 = \frac{1}{2}\left[I_0(\infty) - I_0(0)\right]$$

$$= \frac{1}{2}\left[K_0(0,\infty,\infty) - K_0(0,-\infty,\infty) - K_0(0,\infty,0) + K_0(0,-\infty,0)\right]$$

$$= \frac{1}{2}\left[0 - 0 + 1 + 1\right] = 1 \qquad (54)$$

as a simple example.

3.2 First Collision Probability, $\varepsilon_1 > 0$

For a finite energy cut-off as in Equation (8) the first collision probability is (compare Equation 25a)

$$P_I = \left[\int_0^{\frac{1}{2}\sqrt{\frac{2\epsilon_1}{\mu^*}}} \int_{v_{0_1}}^{\infty} + \int_{\frac{1}{2}\sqrt{\frac{2\epsilon_1}{\mu^*}}}^{\infty} \left\{\int_{v_{0_1}}^{u_0} \frac{1}{2}\left(1 + \frac{v_0}{u_0}\right) + \int_{u_0}^{\infty}\right\}\right] HG\, dv_0\, du_0 \qquad (55)$$

in which $v_{0_1} = \sqrt{\frac{2\epsilon_1}{\mu^*}} - u_0$ is the cut-off locus. Now

$$\sqrt{\frac{2\epsilon_1 \chi_g}{\mu^*}} = \sqrt{(1+\mu)\bar{\epsilon}_1} \quad (= \epsilon^*, \text{ say})$$

$$\sqrt{\frac{2\epsilon_1 \chi_2}{\mu^*}} = \sqrt{\frac{(1+\mu)\bar{\epsilon}_1}{\mu T}} \quad (= \epsilon^* T^*, \text{ say}) \qquad (56)$$

Equation (55) in nondimensional form analogous to Equation (42) then reduces to

$$P_I = \frac{4}{\pi^{1/2}}\left[\int_0^{\frac{\epsilon^*}{2}} \int_{\bar{v}_{0_1}}^{\infty} L_0 + \int_{\frac{\epsilon^*}{2}}^{\infty} \left\{\int_{\bar{v}_{0_1}}^{T^*\bar{u}_0} \frac{1}{2}\left(L_0 + \frac{L_1}{T^*}\right) + \int_{T^*\bar{u}_0}^{\infty} L_0\right\}\right] dv_0\, du_0 \qquad (57)$$

where

$$I_j = \bar{v}_0^{\,j} e^{-\bar{v}_0^2} \bar{u}_0^{\,(3-j)} e^{-\bar{u}_0^2} \tag{58}$$

and

$$\bar{v}_{0_i} = T^*\left(-\bar{u}_0 + \epsilon^*\right) \tag{59}$$

Equivalently, for the three regions a, b, and c as shown in Figure 3:

$$(P_I)_a = \left[I_0\left(\frac{\epsilon^*}{2}\right) - I_0(0) \right]_{-T^*, T^*\epsilon^*}^{0,\infty}$$

$$(P_I)_b = \frac{1}{2}\left\{ \left[I_0(\infty) - I_0\left(\frac{\epsilon^*}{2}\right)\right]_{-T^*, T^*\epsilon^*}^{T^*,0} + \left[I_1(\infty) - I_1\left(\frac{\epsilon^*}{2}\right)\right]_{-T^*, T^*\epsilon^*}^{T^*,0} \right\} \tag{60}$$

$$(P_I)_c = \left[I_0(\infty) - I_0\left(\frac{\epsilon^*}{2}\right) \right]_{T^*,0}^{0,\infty}$$

and the P_I (ϵ^*, T^*) dependence may be interpreted as P_I (μ, $\bar{\epsilon}_1$, $\bar{T}$) on the basis of Equation (56). Thus the corresponding energy and temperature ratio pairs for specific collision probability are

$$\begin{aligned} (\bar{\epsilon}_1)_b &= \frac{1+\mu_a}{1+\mu_b} (\bar{\epsilon}_1)_a \\ \bar{T}_b &= \frac{\mu_a}{\mu_b} \bar{T}_a \end{aligned} \tag{61}$$

for distinct particles μ_a and μ_b.

3.3 Overall Second Collision Probability, $\epsilon_1 > 0$ $\epsilon_2 > 0$

P_{II} follows from Equation (37) modified for finite cut-off energy levels. For example, for $\mu < 3$, i.e. for $dv_{0_2}/du_0 > 0$ for the ϵ_2 cut-off locus defined by Equation (17), two types of integration regions

provide contributions to P_{II}. These will be referred to as Type A and B_i regions, and in each case the result will be seen to depend upon the relative cut-off energy ratio, $\varepsilon_2/\varepsilon_1$, that implies limitations on the relevant portions of the regions (Figure 4). Region boundaries consist of the v_{o_1} and v_{o_2} cut-off locii, and the natural boundaries implied by P_2 as in Equation (37), i.e., $v_o = k_i u_o$ with $k_i = (\mu - 1)/2$, $(3\mu - 1)/4$, 1 and μ.

The contribution from Region A, for which $k_1 = (\mu - 1)/2$ depends upon the relative positions

$$\frac{1}{2}\left(\sqrt{\frac{\bar{\varepsilon}_1}{\bar{\varepsilon}_1}} + \frac{3-\mu}{1+\mu}\right)\epsilon^* = (\bar{u}_o)_a \lesseqgtr (\bar{u}_o)_{b_1} = \frac{\epsilon^*}{1+k_1} \tag{62}$$

or, in general for any k_i,

$$\frac{\bar{\varepsilon}_2}{\bar{\varepsilon}_1} \lesseqgtr \left(\frac{2}{1+k_i} - \frac{3-\mu}{1+\mu}\right)^2 \left[= \left(\frac{\bar{\varepsilon}_2}{\bar{\varepsilon}_1}\right)_{i,\text{say}}\right] \tag{63}$$

and for k_1, $(\bar{\varepsilon}_2/\bar{\varepsilon}_1) \lesseqgtr 1$. Thus

$$\left(P_{II}\right)_{\substack{\text{REGION A} \\ \left(\frac{\bar{\varepsilon}_2}{\bar{\varepsilon}_1} < 1\right)}} = \frac{4}{\pi^{n_2}} \int_{\frac{2\epsilon^*}{1+\mu}}^{\infty} \int_{\bar{v}_{o_1}}^{\frac{\mu+1}{2}\bar{u}_o} \frac{1}{2}\left(L_o + \frac{L_1}{T^*}\right) d\bar{v}_o \, d\bar{u}_o \tag{64a}$$

and

$$\left(P_{II}\right)_{\substack{\text{REGION A} \\ \left(\frac{\bar{\varepsilon}_2}{\bar{\varepsilon}_1} > 1\right)}} = \frac{4}{\pi^{n_2}} \left[\int_{\bar{u}_{o_a}}^{\bar{u}_{o_c}} \int_{\bar{v}_{o_1}}^{\bar{v}_{o_2}} + \int_{\bar{u}_{o_c}}^{\infty} \int_{\bar{v}_{o_1}}^{\frac{\mu+1}{2}\bar{u}_o} \right] \frac{1}{2}\left(L_o + \frac{L_1}{T^*}\right) d\bar{v}_o \, d\bar{u}_o \tag{64b}$$

The contribution from a Region B_i requires consideration of $(\bar{\varepsilon}_2/\bar{\varepsilon}_1)$ relative to both $(\bar{\varepsilon}_2/\bar{\varepsilon}_1)_i$ and $(\bar{\varepsilon}_2/\bar{\varepsilon}_1)_{i+1}$. Thus

$$(P_{II})_{\text{REGION } B_i} = \frac{4}{\pi^{1/2}}\left[\int_{\epsilon^*/1+k_{i+1}}^{\epsilon^*/1+k_i}\int_{\bar{v}_{01}}^{k_{i+1}\bar{T}^*\bar{u}_0} + \int_{\epsilon^*/1+k_i}^{\infty}\int_{k_i\bar{T}^*\bar{u}_0}^{k_{i+1}\bar{T}^*\bar{u}_0}\right] S\, d\bar{v}_0 d\bar{u}_0 \quad (65a)$$

$$\left(\frac{\bar{\varepsilon}_2}{\bar{\varepsilon}_1} < \left(\frac{\bar{\varepsilon}_2}{\bar{\varepsilon}_1}\right)_{i+1}\right)$$

and depending upon $(\bar{u}_0)_c \lesseqgtr (\bar{u}_0)_{bi}$ either:

$$(P_{II})_{\text{REGION } B_i} = \frac{4}{\pi^{1/2}}\left[\int_{\bar{u}_{0a}}^{\bar{u}_{0c}}\int_{\bar{v}_{01}}^{\bar{v}_{02}} + \int_{\bar{u}_{0c}}^{\frac{\epsilon^*}{1+k_i}}\int_{\bar{v}_{01}}^{k_{i+1}\bar{T}^*\bar{u}_0} + \int_{\frac{\epsilon^*}{1+k_i}}^{\infty}\int_{k_i\bar{T}^*\bar{u}_0}^{k_{i+1}\bar{T}^*\bar{u}_0}\right] S\, d\bar{v}_0 d\bar{u}_0 \quad (65b)$$

$$\left(\frac{\bar{\varepsilon}_2}{\bar{\varepsilon}_1}\right)_{i+1} < \frac{\bar{\varepsilon}_2}{\bar{\varepsilon}_1} < \left(\frac{\bar{\varepsilon}_2}{\bar{\varepsilon}_1}\right)_i \quad \text{and} \quad \bar{\varepsilon}_2/\epsilon_1 < E$$

or:

$$(P_{II})_{\text{REGION } B_i} = \frac{4}{\pi^{1/2}}\left[\int_{\bar{u}_{0a}}^{\frac{\epsilon^*}{1+k_i}}\int_{\bar{v}_{01}}^{\bar{v}_{02}} + \int_{\frac{\epsilon^*}{1+k_i}}^{\bar{u}_{0c}}\int_{k_i\bar{T}^*\bar{u}_0}^{\bar{v}_{02}} + \int_{\bar{u}_{0c}}^{\infty}\int_{k_i\bar{T}^*\bar{u}_0}^{k_{i+1}\bar{T}^*\bar{u}_0}\right] S\, d\bar{v}_0 d\bar{u}_0 \quad (65c)$$

$$\left(\frac{\bar{\varepsilon}_2}{\epsilon_1}\right)_{i+1} < \frac{\bar{\varepsilon}_2}{\bar{\varepsilon}_1} < \left(\frac{\bar{\varepsilon}_2}{\bar{\varepsilon}_1}\right)_i \quad \text{and} \quad \bar{\varepsilon}_2/\epsilon_1 > E$$

and

$$(P_{II})_{\text{REGION } B_i} = \frac{4}{\pi^{1/2}}\left[\int_{\bar{u}_{0e}}^{\bar{u}_{0c}}\int_{k_i\bar{T}^*\bar{u}_0}^{\bar{v}_{02}} + \int_{\bar{u}_{0c}}^{\infty}\int_{k_i\bar{T}^*\bar{u}_0}^{k_{i+1}\bar{T}^*\bar{u}_0}\right] S\, d\bar{v}_0 d\bar{u}_0 \quad (65d)$$

$$\left(\frac{\bar{\varepsilon}_2}{\epsilon_1}\right)_i < \frac{\bar{\varepsilon}_2}{\epsilon_1}$$

where

$$S = \frac{P}{T^{*2}} L_2 + \frac{Q}{T^*} L_1 + R L_0$$

$$E = \left(\frac{(3\mu-1) - (3-\mu) k_{i+1}}{(1+\mu)(1+k_i)} \right)^2$$

Also, $\bar{u}_{oa}$ and $\bar{v}_{o1}$ are given by Equations (62) and (59), and the remaining limits are:

$$\begin{aligned} \bar{v}_{o2} &= \frac{T^*}{3-\mu} \left[(3\mu-1)\bar{u}_o - (1+\mu)\epsilon^* \sqrt{\frac{\bar{\epsilon}_2}{\bar{\epsilon}_1}} \right] \\ \bar{u}_{oc} &= \frac{(1+\mu)\epsilon^* \sqrt{\bar{\epsilon}_2/\bar{\epsilon}_1}}{(3\mu-1) - (3-\mu) k_{i+1}} \\ \bar{u}_{oe} &= \frac{(1+\mu)\epsilon^* \sqrt{\bar{\epsilon}_2/\bar{\epsilon}_1}}{(3\mu-1) - (3-\mu) k_i} \end{aligned} \tag{66}$$

Since

$$1 = \left(\frac{\bar{\epsilon}_2}{\bar{\epsilon}_1}\right)_1 > \left(\frac{\bar{\epsilon}_2}{\bar{\epsilon}_1}\right)_j \qquad (j>1) \tag{67}$$

it follows that for $(\bar{\epsilon}_2/\bar{\epsilon}_1) > 1$ only Equations (64b) and (65d) need be considered. The minimum energy criterion entering into Equation (65) is that corresponding to the $v_o = \mu u_o$ upper bound (see Equations (38) and (39), e.g.) for which

$$\left(\frac{\bar{\epsilon}_2}{\bar{\epsilon}_1}\right)_{k_i=\mu} = \left(\frac{\mu-1}{\mu+1}\right)^2 = \begin{cases} 0.0204 & (\mu = 4/3) \\ 0.207 & (\mu = 8/3) \end{cases} \tag{68}$$

from Equation (63). For lesser energy ratios only Equations (64a) and (65a) need be considered and the resulting $P_{II} \neq P_{II}(\bar{\epsilon}_2)$.

For the special case of $(\bar{\epsilon}_2/\bar{\epsilon}_1) > 1$ Equations (64b) and (65d) reduce to:

$$P_{II_A} = 1/2 \left\{ \begin{array}{l} \left[I_0(\bar{u}_{oc}) - I_0(\bar{u}_{oa}) + I_1(\bar{u}_{oc}) - I_1(\bar{u}_{oa}) \right]_{-T^*,\, T^*\epsilon^*}^{\frac{3\mu-1}{3-\mu}T^*,\, -\frac{1+\mu}{3-\mu}T^*\epsilon^*\sqrt{\frac{\bar{\epsilon}_2}{\epsilon_1}}} \\ \\ \left[I_0(\infty) - I_0(\bar{u}_{oc}) + I_1(\infty) - I_1(\bar{u}_{oc}) \right]_{-T^*,\, T^*\epsilon^*}^{\frac{\mu-1}{2}T^*,\, 0} \end{array} \right\} \quad (69)$$

and

$$P_{II_{B\,i}} = \left\{ \begin{array}{l} \left\{ \begin{array}{l} P_i \left[I_2(\bar{u}_{oc}) - I_2(\bar{u}_{oe}) \right] \\ \quad + Q_i \left[I_1(\bar{u}_{oc}) - I_1(\bar{u}_{oe}) \right] + R_i \left[I_0(\bar{u}_{oc}) - I_0(\bar{u}_{oe}) \right] \end{array} \right\}_{k_i T^*,\, 0}^{\frac{3\mu-1}{3-\mu}T^*,\, -\frac{1+\mu}{3-\mu}T^*\epsilon^*\sqrt{\frac{\bar{\epsilon}_2}{\epsilon_1}}} \\ \\ \left\{ \begin{array}{l} P_i \left[I_2(\infty) - I_2(\bar{u}_{oc}) \right] \\ \quad + Q_i \left[I_1(\infty) - I_1(\bar{u}_{oc}) \right] + R_i \left[I_0(\infty) - I_0(\bar{u}_{oc}) \right] \end{array} \right\}_{k_i T^*,\, 0}^{k_{i+1} T^*,\, 0} \end{array} \right\} \quad (70)$$

From Equations (38), (39), and (63), for the specific mass ratios of interest here:

Region B_i	$\mu = 4/3$ k_i	P_i	Q_i	R_i	$\left(\frac{\bar{\epsilon}_2}{\epsilon_1}\right)_{i+1}$	$\mu = 8/3$ k_i	P_i	Q_i	R_i	$\left(\frac{\bar{\epsilon}_2}{\epsilon_1}\right)_{i+1}$
B_1	$\frac{\mu-1}{2} = \frac{1}{6}$	$\frac{1}{4}$	$\frac{-3}{7}$	$\frac{9}{28}$	0.184	$\frac{\mu-1}{2} = \frac{5}{6}$	$\frac{1}{4}$	$\frac{-3}{11}$	$\frac{21}{44}$	0.826
B_2	$\frac{3\mu-1}{4} = \frac{3}{4}$	$\frac{-5}{28}$	$\frac{9}{28}$	0	0.0816	1	0	$\frac{-3}{11}$	$\frac{8}{11}$	0.207
B_3	1	0	$\frac{-3}{7}$	$\frac{4}{7}$	0.0204					

In general, $P_{II} = P_{II}\ (\varepsilon^*, T^*, \mu, \bar{\varepsilon}_2/\bar{\varepsilon}_1)$, and

$$P_{II} = P_{II_A} + \sum_i P_{II_{B_i}} \tag{71}$$

The results for P_I, Equation (60), and P_{II}, Equations (64), (65), were programmed for numerical evaluation over a range of $\bar{\varepsilon}_i$ and $\bar{T}$ for $\mu = 4/3$ and $8/3$. The computer listings are provided in Appendix 1.

CHAPTER 4

DISCUSSION

4.1 Reaction Rates and Energy Cut-offs.

A reaction probability may be defined as[4]

$$\varepsilon_R = \frac{\text{carbon atom flux from surface}}{\text{incident oxygen flux to surface}} \tag{72}$$

and implies maximum $(\varepsilon_R)_0$, $(\varepsilon_R)_{0_2}$ values equal to 1 and 2 respectively for atomic and molecular beams which result in CO as the reaction product. The results of Liu's[4] measurements are given in Table 1 and $(\varepsilon_R)_0$ and $(\varepsilon_R)_{0_2}/2$ may be compared with the collision interaction energy probabilities outlined in Chapter 3 as a measure of the energy constraint importance for effective interactions.

Liu used an oxygen beam at $\theta = 45°$ incidence on a graphite target at temperatures in the range $900 \leq T_s, °K \leq 1800$. From beam temperatures of $T_g = 300$, 1475, 1875, and 2200° K, he inferred the separate atomic and molecular reaction probabilities, $(\varepsilon_R)_0$ and $(\varepsilon_R)_{0_2}$, the dissociated case being based on the highest beam temperature (2200° K) for which the Knudsen source provided a 15% equilibrium dissociation level. Table 1 indicates $(\varepsilon_R)_{0_2}$ to have a primary dependence on surface temperature, T_s, for the appreciable gas temperature, T_g, range considered.

The probability of an encounter with minimum interaction energies $\bar{\varepsilon}_l, \bar{\varepsilon}_j$, is of the form $P(\bar{\varepsilon}_l, \bar{T}, \mu, \bar{\varepsilon}_j/\bar{\varepsilon}_l)$, with the normalized energy referred to T_g as in Equation (11).

For $\theta = 45°$ this implies

$$\varepsilon_i = (0.993 \times 10^{-3})(T_g, °K)\bar{\varepsilon}_i \approx (10^{-3}T_g)\bar{\varepsilon}_1 \text{ kcal/mole} \qquad (73)$$

and therefore provides some indication of cutoff energy level, $\bar{\varepsilon}_i$, variations with T_g if constant ε_i are indeed governing for any collision.

4.2 Collision Probability Results.

The fundamental first collision probability, $P_I(\bar{\varepsilon}_1, \bar{T}, \mu)$ is shown in Fig. 5 for $\mu = 4/3$. Tabulations of the calculated results for all figures are included in Tables 2 through 5. The probability of achieving a given energy cutoff decreases with increasing $\bar{\varepsilon}_i$, and decreasing $\bar{T}$ as follows from the implicit (decreasing T_g, fixed T_s) and (decreasing T_s, fixed T_g) bases respectively. Of interest first is the resulting range $1.0 > P_I > 0.1$ corresponding to $\bar{\varepsilon}_1 \gtrsim 5$, or $\varepsilon_1 \sim$ O(10 kcal/mole) from Equation (73). Secondly, the probability variation near $\bar{T} \sim O(1)$ proves to be quite appreciable but provides no basis for a peak reaction level as is evident from the measurements.

However, increasing $\bar{T}$ implies relatively larger v_o magnitudes for all interactions, and Equation (15) then implies that a lesser number of subsequent collisions may then be attainable. I.e., the larger negative velocity imparted to gas particles results in a larger number of escapes prior to being overtaken by a rebounding surface particle. Fig. 6 indicates the effect on P_{II} of a minimum combined constraint for two collisions, $(\bar{\varepsilon}_1, \bar{\varepsilon}_2) = (0, 0)$, and suggests a resulting basis for the appearance of a peak probability if a multiple interaction is in fact a necessity to affect a reaction. Similarly, the (1,0) and (10^{-3}, 1) constant $\bar{\varepsilon}_i$ locii indicate the scale of the interaction to be as small as O(1) kcal/mole in such cases if $P > 0.1$.

Figures 7 and 8 show the peak development explicitly. For small $\bar{T}$, $\bar{\varepsilon}_1$ dominates, whereas for large $\bar{T}$, $\bar{\varepsilon}_2$ dominates. For the two collision model peaking occurs for $\bar{T} \sim 0(1)$ for energy levels up to $\varepsilon_i \sim 0(10)$ kcal/mole. Clearly an increasing number of collisions implies sharper peaks and their occurrence at lesser $\bar{T}$.

Figures 9 and 10 indicate similar P_I and P_{II} probabilities for $\mu = 8/3$. The lesser $(\varepsilon_R)_{O_2}$ values result in larger $\bar{\varepsilon}_i$ choices but qualitatively similar behavior. Larger mass ratio, however, implies a shift of peak probabilities to relatively larger $\bar{T}$ levels, as must be expected from the increasing demands on v_0 in the inequality Equation (15).

4.3 Energy Levels.

Some activation energies reported for the atomic oxidation of graphite are as follows:[14]

°K	kcal/mole
to 900	0
473 - 573	0-10
488 - 573	6.5
287 - 473	10
293 - 573	1-13

For molecular oxidation the comparable activation energy[15] is in the range 55-65 kcal/mole.

Figure 5 shows a first collision, constant $\bar{\varepsilon}_1$, probability variation with $\bar{T}$ that is consistent with the increasing experimental reactivity up to T $\approx$1300° K., and Figures 6-8 indicate marked reductions in probability for any accompanying second collision. The fit with expe-

riment of the calculated $\bar{\varepsilon}_1 \approx 2.5$ locus corresponds to 5.5 kcal/mole and is in reasonable agreement with the above reported energies[14] for $\mu = 4/3$.

The several data groups obtained for distinct T_g beams in the $\mu = 8/3$ molecular case imply first collision energy level requirements of magnitude (Fig. 10):

T_g	$\approx \bar{\varepsilon}_1$	$\bar{\varepsilon}_1$, kcal/mole
300	30	9.
1475	9	13.
1875	7	13.

The approximately constant ε_1 values above confirm the expected shift of experimental data with $\bar{T}$. This appears to add some importance to the first collision energy criteria.

For both atomic and molecular oxidation it is evident that multiple collisions are required for consistency with a decreased reactivity at higher surface temperatures. This is not totally inconsistent as well, with suggestions of surface annealing and activation[2,16] as competing processes that tend to dominate the reaction control at high and low surface temperatures respectively. A less reactive surface at higher temperatures necessarily should require either a greater first collision energy cut-off or represent a longer dwell time on the surface during which further collisions can take place. These results indicate a marked decrease in probability must be expected if a second collision is required. For example, for $\mu = 4/3$ and near the peak reaction probability ($T_s \approx 1300°$ K) temperature, $P_I(2.5) \approx 2.2$ and $P_{II}(2.5, 0) \approx 0.065$.

4.4 Conclusion.

The probability of encounters between gas and surface particles of sufficient energy provides some of the qualitative features found for oxygen-graphite measured reaction probabilities. Specifically, increased reactivity with increasing surface temperature may be attributed to constant interaction energy constraints, and sharply decreasing reactivity at higher temperatures may be associated with the very much reduced probabilities that follow if any additional collisions are necessary.

APPENDIX 1

COMPUTER LISTINGS

Listings for the individual programs for one and two collision probabilities are given below. In each case only a single input data card is shown (preceding the last deck card, "/*") as an example of the multiple input cards called for by the J = 1, 4 or J = 1, 26 counters.

The symbol equivalence is:

EB	$= \bar{\varepsilon}_1$	TS	$= T^*$
EBR	$= \bar{\varepsilon}_2/\bar{\varepsilon}_1$	UA	$= (\bar{u}_o)a$
EBRI	$= (\bar{\varepsilon}_2/\bar{\varepsilon}_1)_i$	UC	$= (\bar{u}_o)_c$
EBRI1	$= (\bar{\varepsilon}_2/\bar{\varepsilon}_1)_{i+1}$	UE	$= (\bar{u}_o)_e$
ES	$= \varepsilon^*$	V2I	$= \bar{v}_{o_2}(0)$
P1	$= P_I$	V2R	= slope of $\bar{v}_{o_2}(\bar{u}_o)$
P2A	$= (P_{II})_A$	XMU	$= \mu$
P2BB	$= P_{II}$	XKI(j)	$= k_i$
P2B(I)	$= (P_{II})_{Bi}$	XMj	$= M_j$ (j = 0,1,2)
PI	$= P_i$	XK(j + 1)	$= K_j$ (k = 0,1,2)
QI	$= Q_i$	Y	$= y$
RI	$= R_i$	YN	$= N$
TB	$= \bar{T}$		

The two collision listing specifically provides for either of two XMU (= μ) by including the appropriate constants [see table after Equation (70)] in cards labeled 20 to 28.

```
C     ONE COLLISION, BASIC TEST, FINITE D,U
C
      DIMENSION XK(3), XP(8)
      COMMON XK, TS
C     INPUT
      DO 55 J= 1,4
    4 READ 5, XMU,EB,TB
    5 FORMAT (F10.7,2F7.3)
      ES = SQRT ((1. + XMU) * EB)
      ES2 = ES/2.
      TS = 1./SQRT (XMU * TB)
      ET = ES * TS
C
    7 CALL EYEL (-TS,ET,0.,8.,ES2,1,XP(1))
    8 CALL EYEL (-TS,ET,0.,8.,0.0,1,XP(2))
      CALL EYEL (-TS,ET,TS,0.,8.0,1,XP(3))
      CALL EYEL (-TS,ET,TS,0.,ES2,1,XP(4))
      CALL EYEL (-TS,ET,TS,0.,8.0,2,XP(5))
      CALL EYEL (-TS,ET,TS,0.,ES2,2,XP(6))
    9 CALL EYEL (+TS,0.,0.,8.,8.0,1,XP(7))
   10 CALL EYEL (+TS,0.,0.,8.,ES2,1,XP(8))
C
      P1 = XP(1) + (XP(3) + XP(5))/2. + XP(7)
      P1 = P1 - XP(2) - (XP(4) + XP(6))/2. - XP(8)
   35 PRINT 37, XMU,EB,TB,ES,TS
   37 FORMAT (1X,5E20.7//)
      PRINT 40, XP(1), XP(3), XP(5), XP(7)
   40 FORMAT (1X,4E20.7/)
      PRINT 40, XP(2), XP(4), XP(6), XP(8)
      XP(1) = XP(1) - XP(2)
      XP(3) = ( XP(3) - XP(4) ) / 2.
      XP(5) = ( XP(5) - XP(6) ) / 2.
      XP(7) = XP(7) - XP(8)
      PRINT 50, XP(1), XP(3), XP(5), XP(7), P1
   50 FORMAT (1X,5E20.7////)
   55 CONTINUE
      STOP
      END
C
   60 SUBROUTINE EYEL (A,B,C,D,U,L,XI)
      DIMENSION XK(3)
      COMMON XK
      CALL BASIC (C,D,U)
      X1 = XK(L)
      CALL BASIC (A,B,U)
      XI = X1 - XK(L)
      RETURN
      END
C
  350 SUBROUTINE BASIC (G,H,U)
      DIMENSION XK(3)
      COMMON XK, TS
      X2 = SQRT (1. + G*G)
      X3 = (G*H)/X2
      Y = X2*U + X3
      YN = (.88622693) * EXP(-U*U) * ERF(G*U + H)
      X4 = EXP(-(H*H)/(X2*X2))/(2.*X2)
      X5 = (1.7724539)*ERF(Y)
      XM0 = X4 * X5
      IF (Y.LE.12.) GO TO 355
      XM1   =  -(X3 * XM0)/X2
      XM2   = (X5*(1.+2.*X3*X3)*X4) / (2.*X2*X2)
      GO TO 360
  355 XM1 = -(X4*EXP(-Y*Y) + X3*XM0)/X2
      XM2 = 2.*(2.*X3 - Y) * EXP(-Y*Y)
      XM2 = ((XM2 + X5*(1. + 2.*X3*X3))*X4)/(2.*X2*X2)
  360 XK(1) = (1.1283792) * (G*(XM0 + XM2) - YN * (1. + U*U))
      XK(2) = -(XM2 * .5641896)/TS
      XK(3) = ((.5641896)/(TS*TS)) * (G*XM0 - YN - 2.*(H*XM1 + G*XM2))
      RETURN
      END
//G.SYSIN DD *
+2.6666667+04.000+08.000
/*
```

SAMPLE OUTPUT, ONE COLLISION PROGRAM

0.2666667E+01	0.4000000E+01	0.2000000E+01	0.3829709E+01	0.4330126E+00
0.3161365E-01	0.6347336E+00	-0.3638910E+00	-0.5646686E+00	
-0.7241398E-01	0.6181731E+00	-0.3703180E+00	-0.5865594E+00	
0.1040276E+00	0.8280277E-02	0.3213495E-02	0.2189082E-01	0.1374122E+00

```
C      TWO COLLISIONS, XMU INPUT FOR 4/3, 8/3
C
       DIMENSION XK(3), XP(18), P2B(3), PI(3), QI(3), RI(3), XKI(4)
       COMMON  XK,  TS
C      INPUT
       DO 65 J = 1,26
     4 READ 200, XMU,EB,TB,EBR
       ES     = SQRT ( (1. + XMU ) * EB )
       ES2    =  ES/2.
       TS     = 1. / SQRT(XMU*TB)
       ET     =  ES * TS
       EB2    = SQRT (EBR)
       UA     = ( (3.-XMU) / (1. + XMU) + EB2 ) * ES * .5
       V2R    = ( (3. * XMU - 1.) * TS) / (3. - XMU)
       V2I    = -( (1. + XMU) * ES * TS * EB2) / (3. - XMU)
       P2B(3)= 0.
       PRINT 204, XMU, EB, TB, ES, TS, EBR
       PRINT 208
C
     5 Z1     = ( XMU - 1. ) * TS * .5
       IF (EBR.LE.1.) GO TO 10
       UC     = (2. * ES * EB2) / (1. + XMU)
       CALL EYEL (-TS, ET, V2R, V2I, UC, 1, XP(1) )
       CALL EYEL (-TS, ET, V2R, V2I, UA, 1, XP(2) )
       CALL EYEL (-TS, ET, V2R, V2I, UC, 2, XP(3) )
       CALL EYEL (-TS, ET, V2R, V2I, UA, 2, XP(4) )
       CALL EYEL (-TS, ET, Z1 , 0.0, B., 1, XP(5) )
       CALL EYEL (-TS, ET, Z1 , 0.0, UC, 1, XP(6) )
       CALL EYEL (-TS, ET, Z1 , 0.0, B., 2, XP(7) )
       CALL EYEL (-TS, ET, Z1 , 0.0, UC, 2, XP(8) )
       PRINT 206, XP(1), XP(3), XP(5), XP(7)
       PRINT 206, XP(2), XP(4), XP(6), XP(8)
       DO 6 K1 = 1,7,2
     6 XP(K1)= XP(K1) - XP(K1+1)
       PRINT 206, XP(1), XP(3), XP(5), XP(7)
       P2A    = ( XP(1) + XP(3) + XP(5) + XP(7) ) * .5
       PRINT 210, P2A
       GO TO 15
C
    10 Z2     = (2.*ES) / (1.+XMU)
       CALL EYEL (-TS, ET, Z1 , 0. , B., 1, XP(1) )
       CALL EYEL (-TS, ET, Z1 , 0. , Z2, 1, XP(2) )
       CALL EYEL (-TS, ET, Z1 , 0. , B., 2, XP(3) )
       CALL EYEL (-TS, ET, Z1 , 0. , Z2, 2, XP(4) )
       PRINT 212, XP(1), XP(3)
       PRINT 212, XP(2), XP(4)
       XP(1) = XP(1) - XP(2)
       XP(3) = XP(3) - XP(4)
       PRINT 212, XP(1), XP(3)
       P2A    = ( XP(1) + XP(3) ) * .5
       PRINT 214, P2A
C
    15 IF (XMU.GE.3.) GO TO 65
       IF (XMU.LE.1.667) GO TO 25
    20 PI(1) =  1./4.
       PI(2) = 0.
       PI(3) = 0.
       QI(1) = -3./11.
       QI(2) = -3./11.
       QI(3) = 0.
       RI(1) = 21./44.
       RI(2) = 8./11.
       RI(3) = 0.
       XKI(1)= 5./6.
       XKI(2)= 1.0
       XKI(3)= 8./3.
       XKI(4)= 0.
       IL     =  2
       GO TO 28
```

```
C
   25 PI(1) = 1./4.
      PI(2) = -5./28.
      PI(3) = 0.
      QI(1) = -3./7.
      QI(2) = 9./28.
      QI(3) = - 3./7.
      RI(1) = 9./28.
      RI(2) = 0.
      RI(3) = 4./7.
      XKI(1)= 1./6.
      XKI(2)= 3./4.
      XKI(3)= 1.0
      XKI(4)= 4./3.
      IL    =  3
C
   28 PRINT 216, PI
      PRINT 216, QI
      PRINT 216, RI
      PRINT 206, XKI
      PRINT 208
C
      DO 60 I = 1,IL
      EBRI  = ( (2./(1.+XKI(I))) - ((3.-XMU)/(1.+XMU)) ) ** 2.
      EBRI1 = ( (2./(1.+XKI(I+1))) - ((3.-XMU)/(1.+XMU)) ) ** 2.
      TSK   = TS * XKI(I)
      TSK1  = TS * XKI(I+1)
      ESK   = ES / (1.+XKI(I) )
      ESK1  = ES / (1. + XKI(I+1) )
      UC    = ( (1.+XMU)*ES*EB2) / ( (3.*XMU - 1.) - (3.-XMU)*XKI(I+1) )
      UE    = ((1.+XMU)*ES*EB2)/((3.*XMU-1.)-(3.-XMU)*XKI(I))
      PRINT 216, EBRI1, EBR, EBRI
      PRINT 212, UE,UC
C
   30 IF (EBR.GE.EBRI1) GO TO 35
      CALL EYEL (TSK, 0., TSK1, 0., 8.0 , 3, XP(1) )
      CALL EYEL (TSK, 0., TSK1, 0., ESK , 3, XP(2) )
      CALL EYEL (TSK, 0., TSK1, 0., 8.0 , 2, XP(3) )
      CALL EYEL (TSK, 0., TSK1, 0., ESK , 2, XP(4) )
      CALL EYEL (TSK, 0., TSK1, 0., 8.0 , 1, XP(5) )
      CALL EYEL (TSK, 0., TSK1, 0., ESK , 1, XP(6) )
      CALL EYEL (-TS, ET, TSK1, 0., ESK , 3, XP(7) )
      CALL EYEL (-TS, ET, TSK1, 0., ESK1, 3, XP(8) )
      CALL EYEL (-TS, ET, TSK1, 0., ESK , 2, XP(9) )
      CALL EYEL (-TS, ET, TSK1, 0., ESK1, 2, XP(10) )
      CALL EYEL (-TS, ET, TSK1, 0., ESK , 1, XP(11) )
      CALL EYEL (-TS, ET, TSK1, 0., ESK1, 1, XP(12) )
      PRINT 218
      GO TO 38
C
   35 IF (EBR.LE.EBRI) GO TO 45
      CALL EYEL (TSK, 0., TSK1, 0.0, 8., 3, XP(1) )
      CALL EYEL (TSK, 0., TSK1, 0.0, UC, 3, XP(2) )
      CALL EYEL (TSK, 0., TSK1, 0.0, 8., 2, XP(3) )
      CALL EYEL (TSK, 0., TSK1, 0.0, UC, 2, XP(4) )
      CALL EYEL (TSK, 0., TSK1, 0.0, 8., 1, XP(5) )
      CALL EYEL (TSK, 0., TSK1, 0.0, UC, 1, XP(6) )
      CALL EYEL (TSK, 0., V2R , V2I, UC, 3, XP(7) )
     *CALL EYEL (TSK, 0., V2R , V2I, UE, 3, XP(8) )
      CALL EYEL (TSK, 0., V2R , V2I, UC, 2, XP(9) )
      CALL EYEL (TSK, 0., V2R , V2I, UE, 2, XP(10) )
      CALL EYEL (TSK, 0., V2R , V2I, UC, 1, XP(11) )
      CALL EYEL (TSK, 0., V2R , V2I, UE, 1, XP(12) )
      PRINT 220
   38 PRINT 204, XP(1), XP(3), XP(5), XP(7), XP(9), XP(11)
      PRINT 204, XP(2), XP(4), XP(6), XP(8), XP(10), XP(12)
      DO 40 K1 = 1,11,2
   40 XP(K1) = XP(K1) - XP(K1+1)
      PRINT 204, XP(1), XP(3), XP(5), XP(7), XP(9), XP(11)
      DO 42 K1 = 1,7,6
      XP(K1) = XP(K1) * PI(I)
      XP(K1+2) = XP(K1+2) * QI(I)
   42 XP(K1+4) = XP(K1+4) * RI(I)
```

```
      P2B(I) = XP(1) + XP(3) + XP(5) + XP(7) + XP(9) + XP(11)
      PRINT 226, P2B(I)
      GO TO 60
C
   45 EBRR  =  ((3.*XMU-1.)-(3.-XMU)*XKI(I+1))
      EBRR  = ( EBRR / ((1.+XMU)*(1.+XKI(I))))  ** 2.
      PRINT 222, EBRR
      IF (EBR.GE.EBRR) GO TO 50
      CALL EYEL (TSK, 0., TSK1, 0.0, 8.0, 3, XP(1) )
      CALL EYEL (TSK, 0., TSK1, 0.0, ESK, 3, XP(2) )
      CALL EYEL (TSK, 0., TSK1, 0.0, 8.0, 2, XP(3) )
      CALL EYEL (TSK, 0., TSK1, 0.0, ESK, 2, XP(4) )
      CALL EYEL (TSK, 0., TSK1, 0.0, 8.0, 1, XP(5) )
      CALL EYEL (TSK, 0., TSK1, 0.0, ESK, 1, XP(6) )
      CALL EYEL (-TS, ET, TSK1, 0.0, ESK, 3, XP(7) )
      CALL EYEL (-TS, ET, TSK1, 0.0, UC , 3, XP(8) )
      CALL EYEL (-TS, ET, TSK1, 0.0, ESK, 2, XP(9) )
      CALL EYEL (-TS, ET, TSK1, 0.0, UC , 2, XP(10) )
      CALL EYEL (-TS, ET, TSK1, 0.0, ESK, 1, XP(11) )
      CALL EYEL (-TS, ET, TSK1, 0.0, UC , 1, XP(12) )
      CALL EYEL (-TS, ET, V2R , V2I, UC , 3, XP(13) )
      CALL EYEL (-TS, ET, V2R , V2I, UA , 3, XP(14) )
      CALL EYEL (-TS, ET, V2R , V2I, UC , 2, XP(15) )
      CALL EYEL (-TS, ET, V2R , V2I, UA , 2, XP(16) )
      CALL EYEL (-TS, ET, V2R , V2I, UC , 1, XP(17) )
      CALL EYEL (-TS, ET, V2R , V2I, UA , 1, XP(18) )
      GO TO 55
C
   50 CALL EYEL (TSK,  0., TSK1, 0.0, 8.0, 3, XP(1) )
      CALL EYEL (TSK,  0., TSK1, 0.0, UC , 3, XP(2) )
      CALL EYEL (TSK,  0., TSK1, 0.0, 8.0, 2, XP(3) )
      CALL EYEL (TSK,  0., TSK1, 0.0, UC , 2, XP(4) )
      CALL EYEL (TSK,  0., TSK1, 0.0, 8.0, 1, XP(5) )
      CALL EYEL (TSK,  0., TSK1, 0.0, UC , 1, XP(6) )
      CALL EYEL (TSK,  0., V2R , V2I, UC , 3, XP(7) )
      CALL EYEL (TSK,  0., V2R , V2I, ESK, 3, XP(8) )
      CALL EYEL (TSK,  0., V2R , V2I, UC , 2, XP(9) )
      CALL EYEL (TSK,  0., V2R , V2I, ESK, 2, XP(10) )
      CALL EYEL (TSK,  0., V2R , V2I, UC , 1, XP(11) )
      CALL EYEL (TSK,  0., V2R , V2I, ESK, 1, XP(12) )
      CALL EYEL (-TS, ET, V2R , V2I, ESK, 3, XP(13) )
      CALL EYEL (-TS, ET, V2R , V2I, UA , 3, XP(14) )
      CALL EYEL (-TS, ET, V2R , V2I, ESK, 2, XP(15) )
      CALL EYEL (-TS, ET, V2R , V2I, UA , 2, XP(16) )
      CALL EYEL (-TS, ET, V2R , V2I, ESK, 1, XP(17) )
      CALL EYEL (-TS, ET, V2R , V2I, UA , 1, XP(18) )
   55 PRINT 204, XP(1), XP(3), XP(5), XP(7), XP(9), XP(11)
      PRINT 204, XP(2), XP(4), XP(6), XP(8), XP(10), XP(12)
      PRINT 216, XP(13), XP(15), XP(17)
      PRINT 216, XP(14), XP(16), XP(18)
      PRINT 208
      DO 57 K1 = 1,17,2
   57 XP(K1) = XP(K1) - XP(K1+1)
      PRINT 204, XP(1), XP(3), XP(5), XP(7), XP(9), XP(11)
      PRINT 216, XP(13), XP(15), XP(17)
      DO 59 K1 = 1,13,6
      XP(K1) = XP(K1) * PI(I)
      XP(K1+2) = XP(K1+2) * QI(I)
   59 XP(K1+4) = XP(K1+4) * RI(I)
      P2B(I) = XP(1) + XP(3) + XP(5) + XP(7) + XP(9)
      P2B(I) = XP(11) + XP(13) + XP(15) + XP(17) + P2B(I)
      PRINT 226, P2B(I)
C
   60 CONTINUE
      P2BB  = P2A + P2B(1) + P2B(2) + P2B(3)
      PRINT 224, P2BB
   65 CONTINUE
      STOP
```

```
  200 FORMAT (F10.7,F6.3,E8.1,E11.4)
  204 FORMAT (1X, 6E20.7)
  206 FORMAT (1X, 4E20.7)
  208 FORMAT (1X,//)
  210 FORMAT (1X, 'P2A EBR GREATER THAN ONE =', E20.7//)
  212 FORMAT (1X, 2E20.7)
  214 FORMAT (1X, 'P2A EBR LESS THAN ONE =', E20.7//)
  216 FORMAT (1X, 3E20.7)
  218 FORMAT (1X, 'P2B EBR LESS THAN EBRI1')
  220 FORMAT (1X, 'P2B EBR GREATER THAN EBRI')
  222 FORMAT (1X, 'P2B EBR BRACKETED   EBRR =', E 20.7 )
  224 FORMAT (1X, 'TWO COLLISION PROBABILITY = ', E 20.7/////)
  226 FORMAT (1X, 'P2BI = ', E20.7//)
      END
C
  300 SUBROUTINE EYEL (A,B,C,D,U,L,XI)
      DIMENSION XK(3)
      COMMON XK
      CALL BASIC (C,D,U)
      X1 = XK(L)
      CALL BASIC (A,B,U)
      XI = X1 - XK(L)
      RETURN
      END
C
  350 SUBROUTINE BASIC (G,H,U)
      DIMENSION XK(3)
      COMMON XK, TS
      X2 = SQRT (1. + G*G)
      X3 = (G*H)/X2
      Y = X2*U + X3
      YN = (.88622693) * EXP(-U*U) * ERF(G*U + H)
      X4 = EXP(-(H*H)/(X2*X2))/(2.*X2)
      X5 = (1.7724539)*ERF(Y)
      XM0 = X4 * X5
      IF (Y.LE.12.) GO TO 355
      XM1    =  -(X3 * XM0)/X2
      XM2    = (X5*(1.+2.*X3*X3)*X4) / (2.*X2*X2)
      GO TO 360
  355 XM1 = -(X4*EXP(-Y*Y) + X3*XM0)/X2
      XM2 = 2.*(2.*X3 - Y) * EXP(-Y*Y)
      XM2 = ((XM2 + X5*(1. + 2.*X3*X3))*X4)/(2.*X2*X2)
  360 XK(1) = (1.1283792) * (G*(XM0 + XM2) - YN * (1. + U*U))
      XK(2) = -(XM2 * .5641896)/TS
      XK(3) = ((.5641896)/(TS*TS)) * (G*XM0 - YN - 2.*(H*XM1 + G*XM2))
      RETURN
      END
//G.SYSIN DD *
+1.3333333+0.000+5.0E-01+0.0000E+00
/*
```

SAMPLE OUTPUT, TWO COLLISION PROGRAM

```
      0.2666667E+01       0.4000000E+01       0.2000000E+01       0.3829709E+01       0.4330126E+00       0.1000000E+01


      0.5596462E+00      -0.3982421E+00
      0.5505552E+00      -0.4012299E+00
      0.9090960E-02       0.2987802E-02
P2A EBR LESS THAN ONE =       0.6039381E-02

      0.2500000E+00       0.0                 0.0
     -0.2727273E+00      -0.2727273E+00       0.0
      0.4772727E+00       0.7272727E+00       0.0
      0.8333333E+00       0.1000000E+01       0.2666666E+01       0.0


      0.8264465E+00       0.1000000E+01       0.1000000E+01
      0.2088931E+01       0.2106339E+01
P2B EBR BRACKETED   EBRR =       0.9835399E+00
      0.6303227E-01       0.3435111E-01       0.7508761E-01      -0.6869829E-01       0.4635574E+00      -0.4110028E+00
      0.5876887E-01       0.3202051E-01       0.6997955E-01      -0.6883597E-01       0.4634800E+00      -0.4111779E+00
      0.4557121E+00       0.6225016E-01       0.1393772E+00
      0.4557122E+00       0.6225024E-01       0.1393765E+00


      0.4263401E-02       0.2330601E-02       0.5108058E-02       0.1376867E-03       0.7736683E-04       0.1750588E-03
     -0.1192093E-06      -0.7450581E-07       0.6556511E-06
P2BI =       0.2965344E-02

      0.2066118E+00       0.1000000E+01       0.8264465E+00
      0.2106339E+01       0.2297825E+01
P2B EBR GREATER THAN EBRI
      0.9845816E+00       0.2841735E+00       0.3532450E+00      -0.1203202E+00       0.4342796E+00      -0.4766345E+00
      0.9777294E+00       0.2816131E+00       0.3492690E+00      -0.1274672E+00       0.4315369E+00      -0.4809824E+00
      0.6852150E-02       0.2560377E-02       0.3975987E-02       0.7146955E-02       0.2742708E-02       0.4347861E-02
P2BI =       0.4607409E-02


TWO COLLISION PROBABILITY =       0.1361213E-01
```

TABLE 1

MEASURED REACTION PROBABILITIES

(From Reference 4)

T_s, °K	$(\varepsilon_R)_{O_2}$			$(\varepsilon_R)_O$
	T_g, °K = 300	1475	1875	2200
1000	.0041		.0034	.154
1050		.0045		
1100	.0089		.0079	.192
1150		.0104		
1210	.0149	.0133	.0123	.221
1300				.261
1310	.0158	.0145	.0171	
1400	.0116	.0110	.0130	.271
1510	.0060	.0065	.0081	.221
1600	.0055	.0048	.0055	.175
1700	.0045			.154
1710		.0036		
1720			.0048	

TABLE 2

ONE COLLISION PROBABILITY, $\mu = 4/3$

$\bar{T}$	P_I					
	$\bar{\varepsilon}_1$ = 0.5	1.0	2.0	3.0	4.0	5.0
0.25	.693	.405	.110	.0261	.00575	.00121
0.50	.711	.463	.168	.0548	.0168	.00495
1.00	.741	.541	.267	.123	.0548	.0237
2.00	.783	.630	.397	.243	.146	.9863
4.00	.829	.716	.533	.393	.287	.209
6.00	.854	.761	.605	.480	.380	.299

TABLE 3

TWO COLLISION PROBABILITY, $\mu = 4/3$

$\bar{T}$	$P_{II}(\bar{\varepsilon}_1, 0)$					
	$\bar{\varepsilon}_1 =$ 0	1	1.5	2	3	4
0.1	.872	.307	.145	.0644	.0115	.00188
0.25	.791	.286	.147	.0726	.0164	.00346
0.5	.715	.265	.150	.0828	.0244	.00697
1.0	.623	.239	.148	.0920	.0357	.0140
2.0	.517	.207	.138	.0941	.0453	.0226
4.0	.409	.170	.120	.0864	.0476	.0273
6.0	.350	.148	.106	.0784	.0453	.0274

$\bar{T}$	$P_{II}(\bar{\varepsilon}_1, 1)$				$P_{II}(10^{-3}, \bar{\varepsilon}_2)$	
	$\bar{\varepsilon}_1 =$ 1	2	3	4	$\bar{\varepsilon}_2 =$ 1	2
0.1	.288	.0640	.0115	.00188	.544	.225
0.25	.241	.0669	.0158	.00342	.503	.222
0.5	.201	.0660	.0205	.00620	.460	.217
1.0	.162	.0606	.0235	.00934	.400	.202
2.0	.125	.0512	.0229	.01067	.328	.175
4.0	.0937	.0404	.0195	.00991	.255	.141
6.0	.0781	.0343	.0170	.00891	.215	.120

TABLE 4

ONE COLLISION PROBABILITY, $\mu = 8/3$

$\bar{T}$	P_I			
	$\bar{\varepsilon}_1$ = 4.0	8.0	16.	32.
.5	.00780	.000026	.000000	.000000
1.0	.0431	.00121	.000000	.000000
2.0	.137	.0167	.000217	.000000
4.0	.284	.0833	.00737	.000058
6.0	.379	.154	.0275	.000938
8.0	.445	.216	.0553	.004017

TABLE 5

TWO COLLISION PROBABILITY, $\mu = 8/3$

$\bar{T}$	$P_{II}(\bar{\varepsilon}_1, 0)$			
	$\bar{\varepsilon}_1 =$ 0	3	6	8
.5	.910	.00565	.00032	.00002
1.0	.833	.0230	.00353	.00053
2.0	.732	.0542	.0156	.00450
4.0	.613	.129	.0329	.0135
6.0	.539	.133	.0403	.0186
8.0	.488	.130	.0432	.0212

$\bar{T}$	$P_{II}(\bar{\varepsilon}_1, \bar{\varepsilon}_2)$					
	$\bar{\varepsilon}_1 = 10^{-3}$	4	4	4	8	8
	$\bar{\varepsilon}_2 =$ 4	2	4	8	4	8
.25	.0889		.00084			
.5	.0875	.00529	.00344	.000455	.000016	.000006
1.0	.0834	.01872	.00833	.000629	.000312	.000047
2.0	.0756	.0399	.0136	.000734	.00180	.000137
4.0	.0652	.0581	.0172	.000757	.00457	.000237
8.0	.0537	.0641	.0181	.000708	.00694	.000297
20.0	.0388	.0553	.0156	.000572	.00747	.000294
40.0	.0290	.0438	.0124	.000450	.00641	.000250

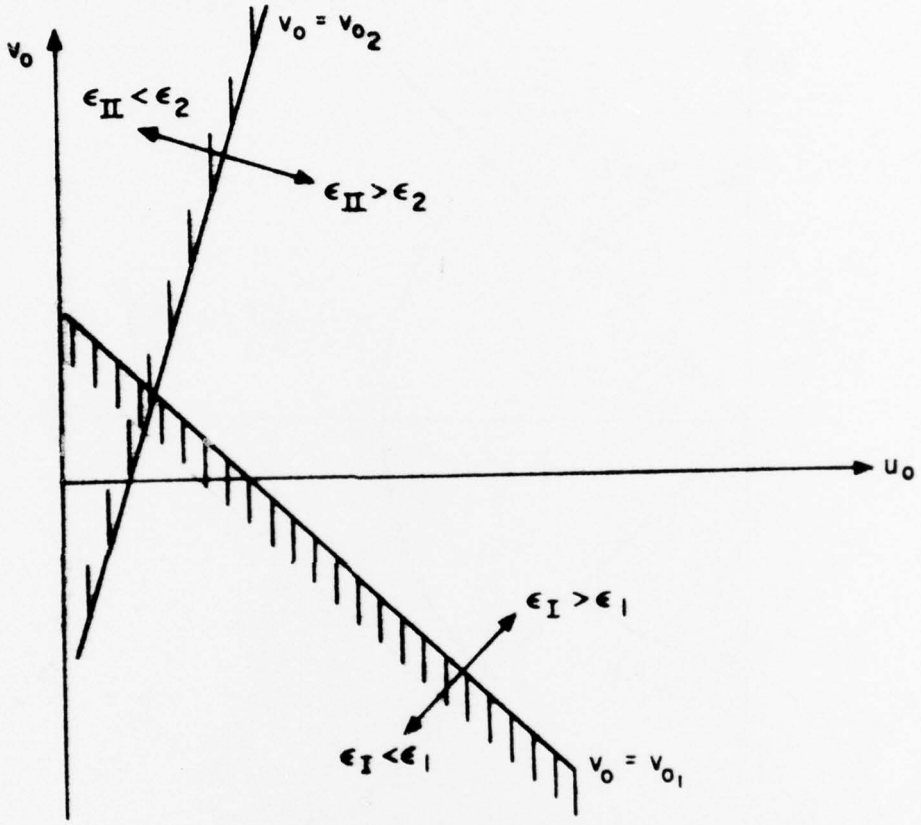

Fig. 1. Energy Constraints for (u_o, v_o) Pairs

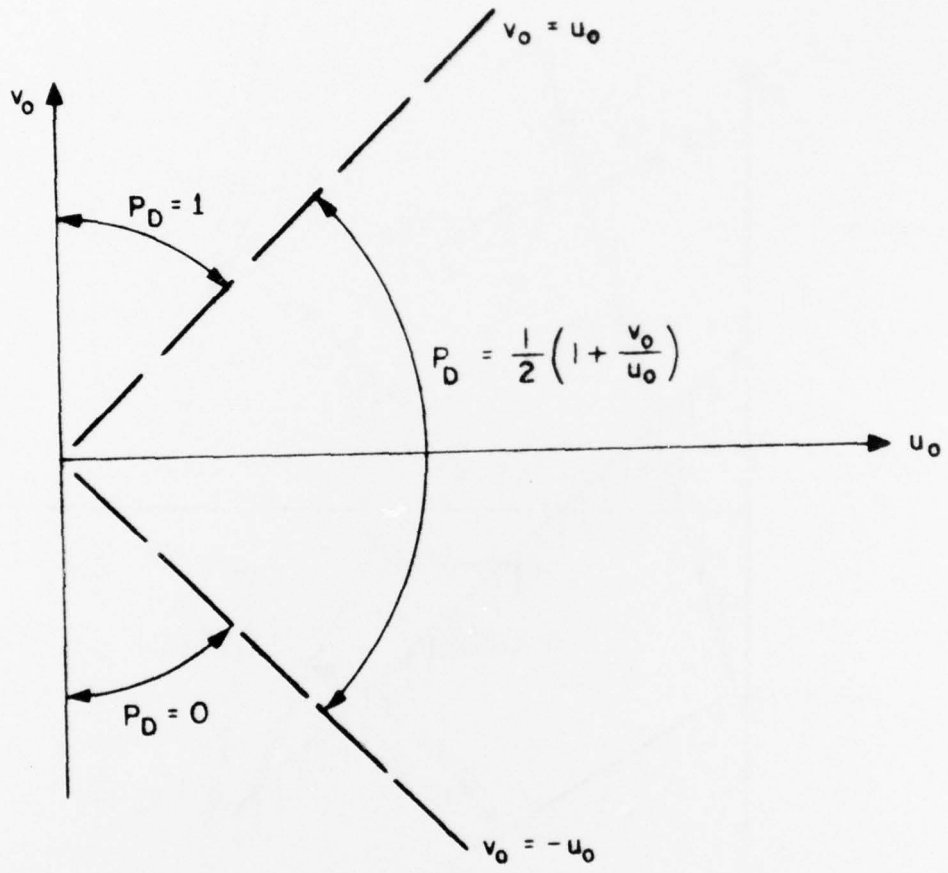

Fig. 2. Directional Probability

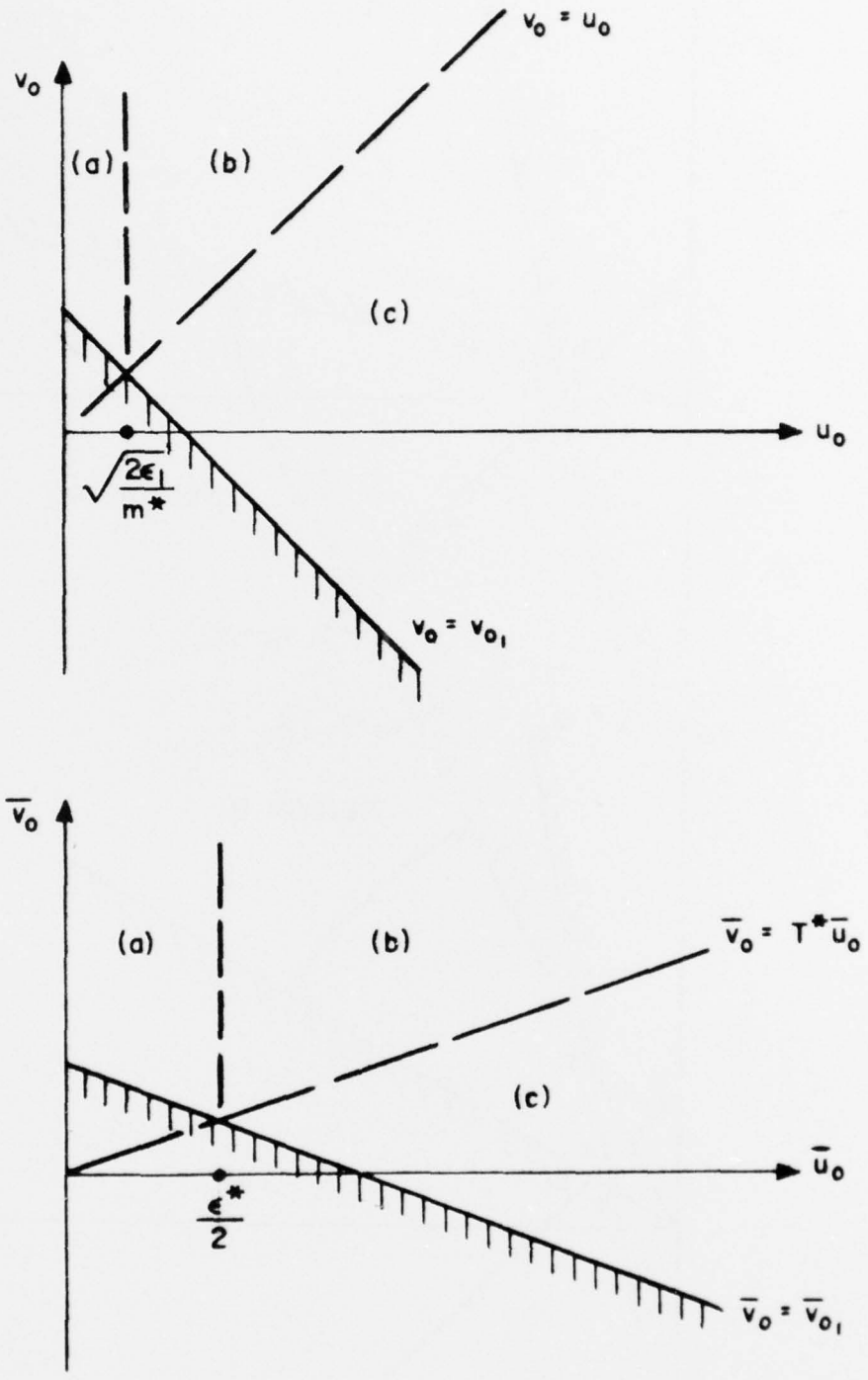

Fig. 3. Integration Regions for First Collision Probability, P_I

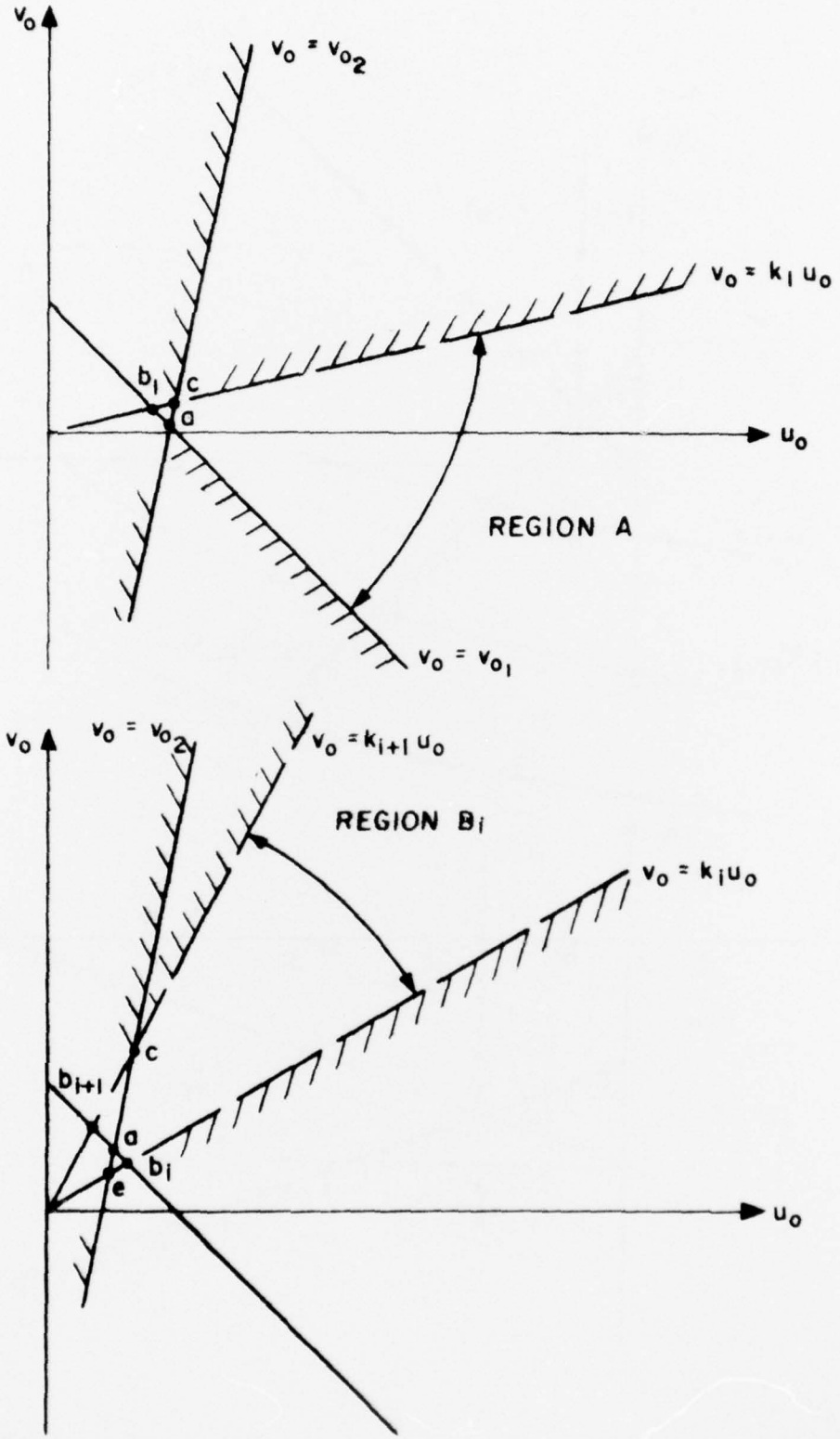

Fig. 4. Integration Regions for Second Collision Probability, P_{II}

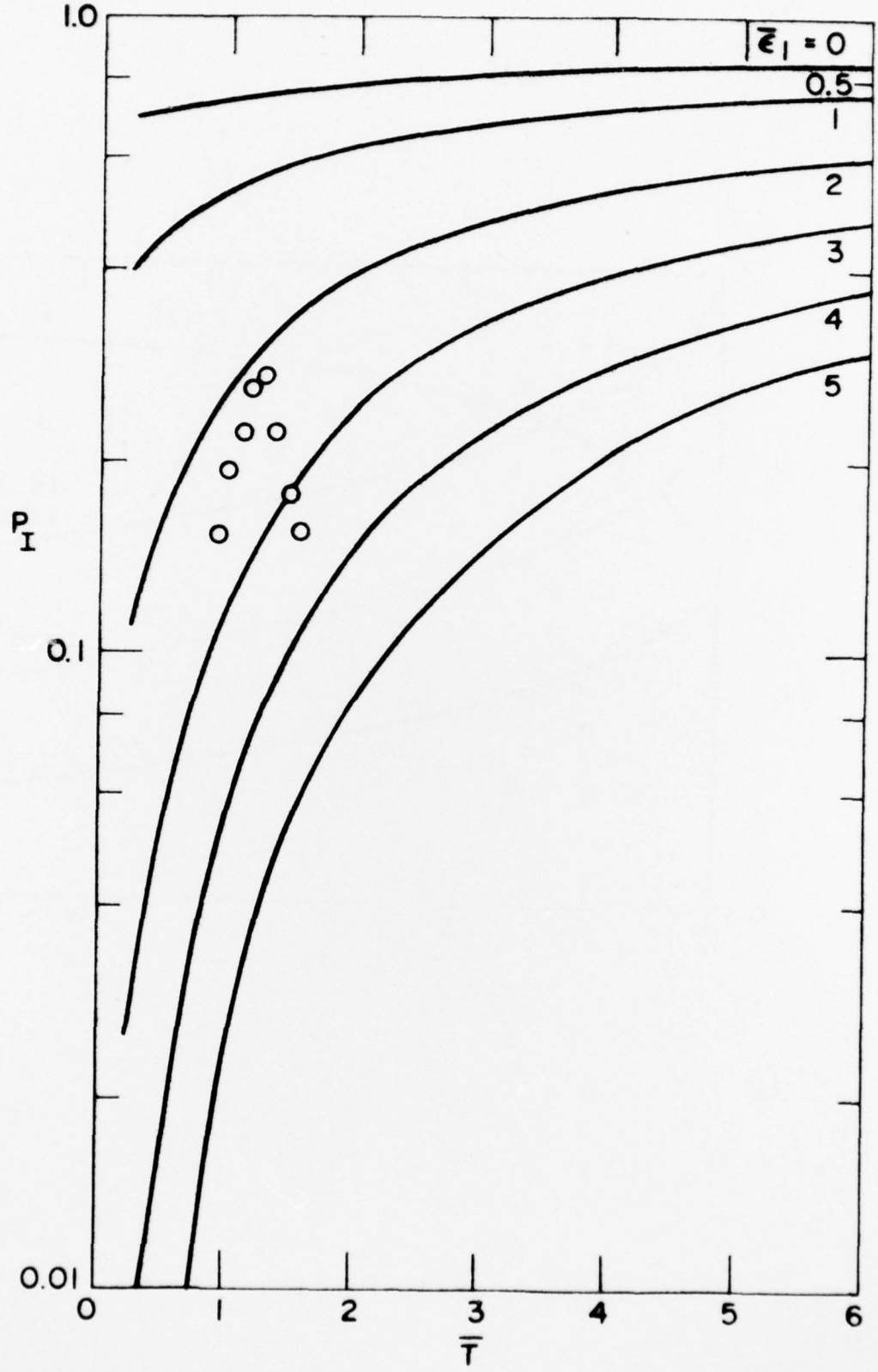

Fig. 5. Single Collision Probability, $\mu = 4/3$, Experiment (O) $T_g = 2200°$ K.

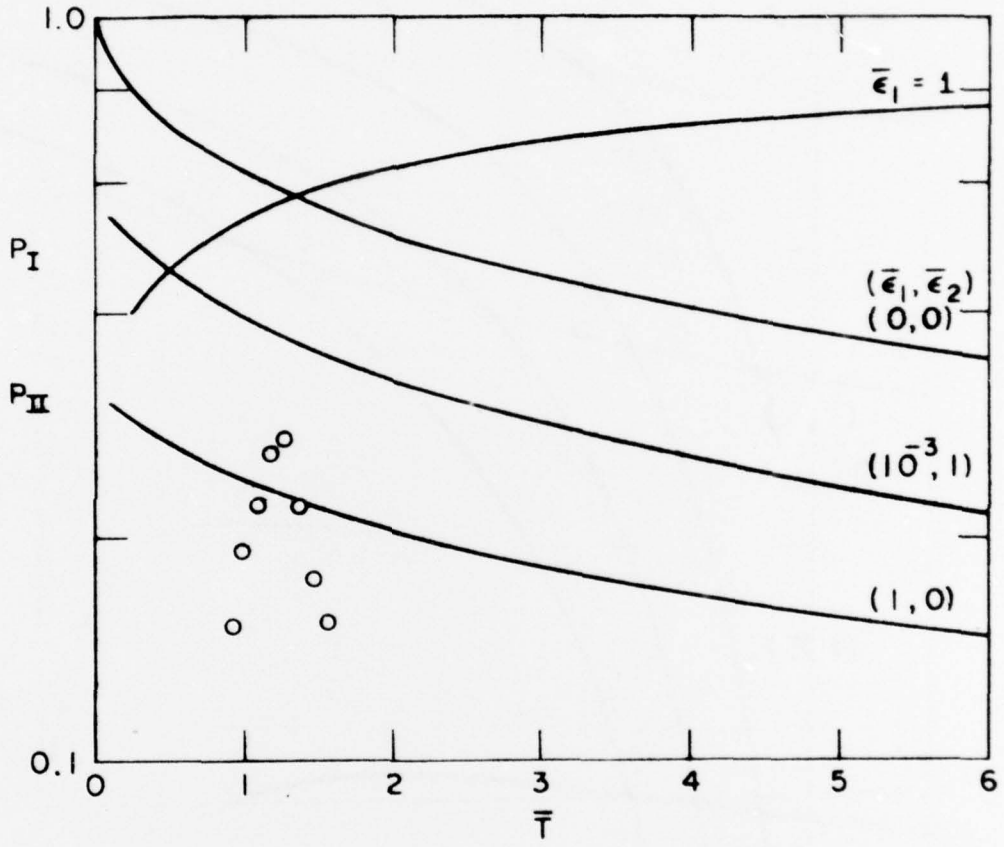

Fig. 6. One and Two Collision Bounds, $\mu = 4/3$

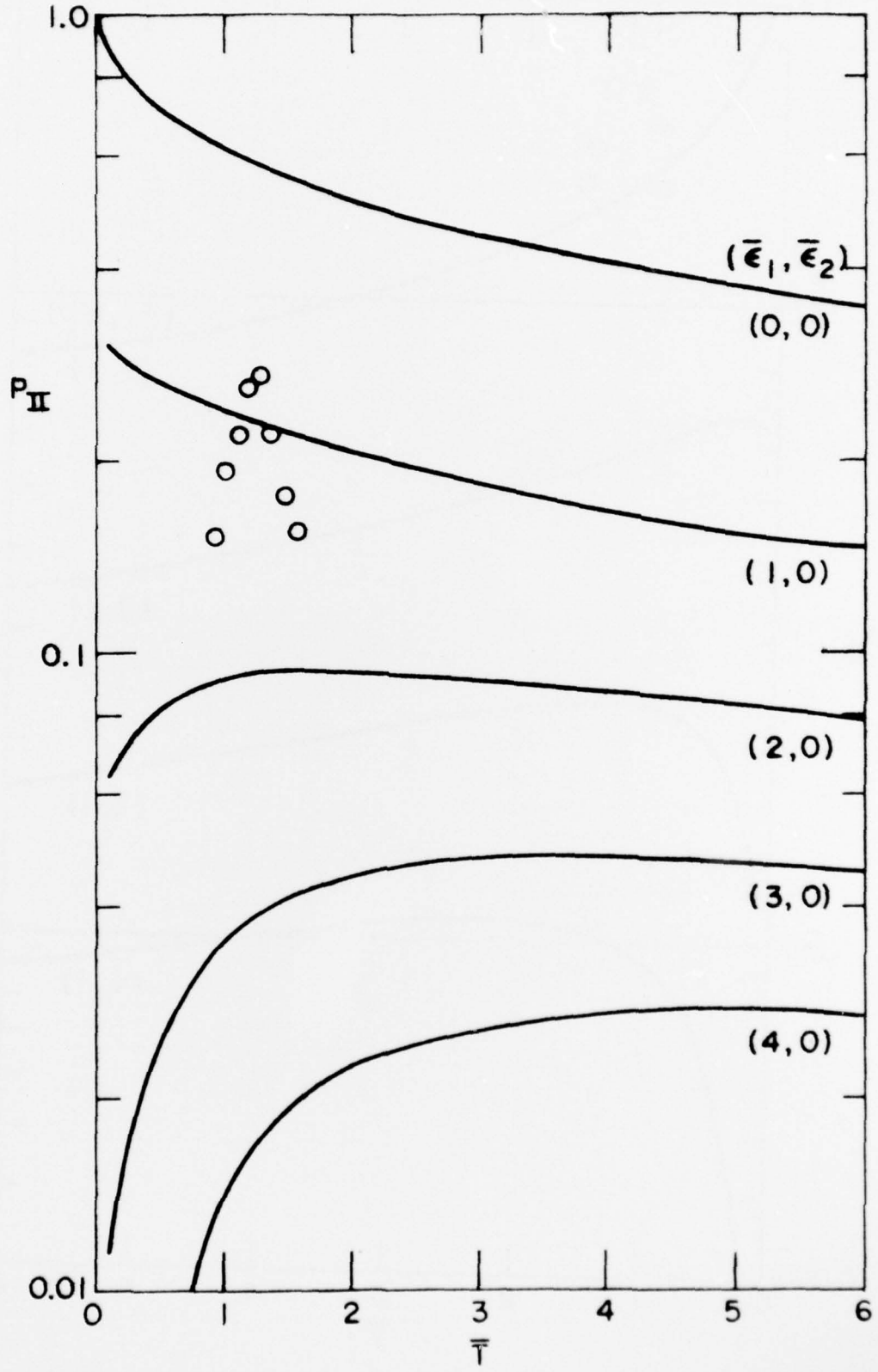

Fig. 7. Two Collision Probability, $\bar{\epsilon}_2 = 0$, $\mu = 4/3$, Experiment (O) $T_g = 2200°$ K.

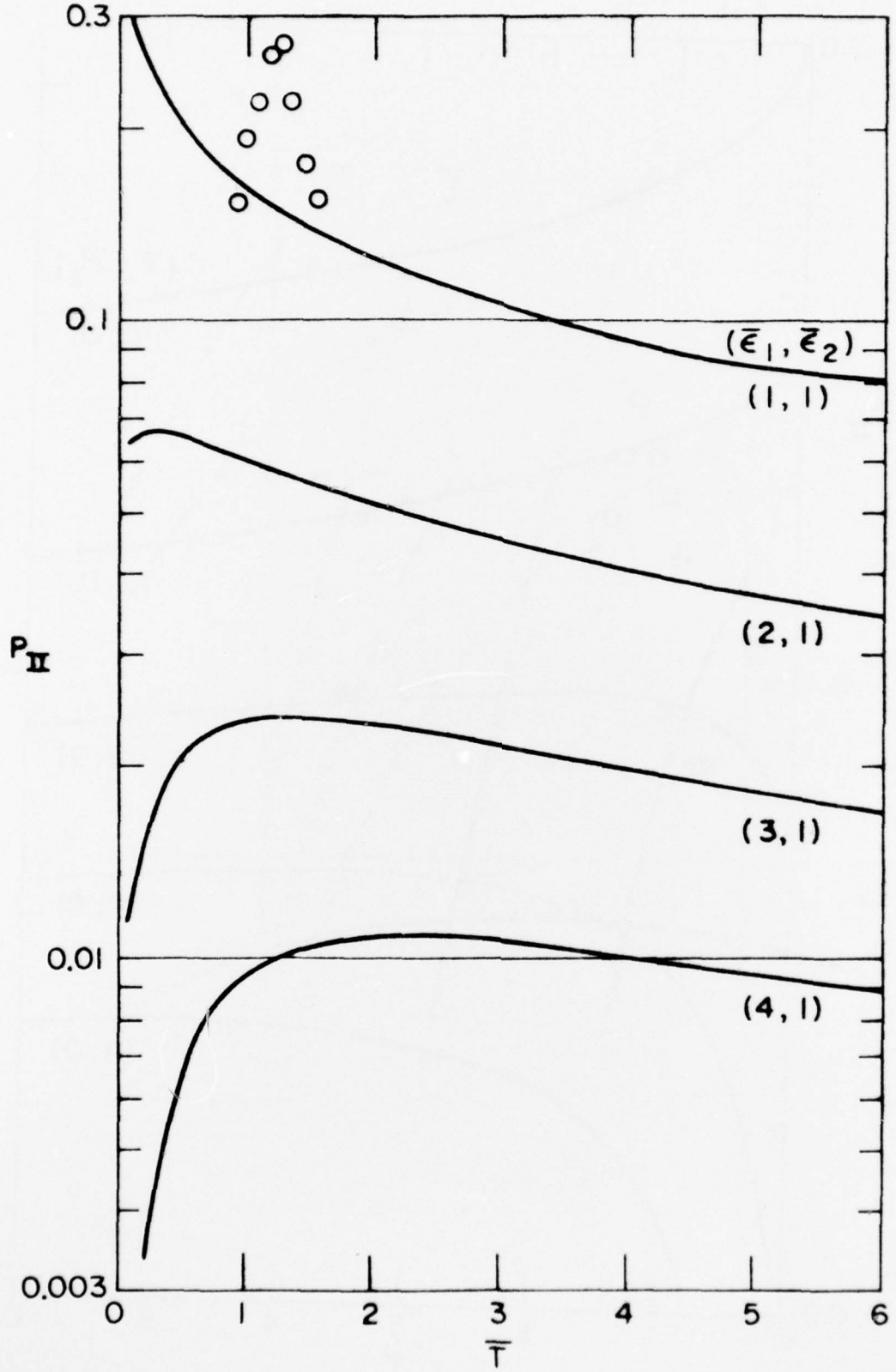

Fig. 8. Two Collision Probability, $\bar{\epsilon}_2 = 1$, $\mu = 4/3$, Experiment (O) $T_g = 2200°$ K.

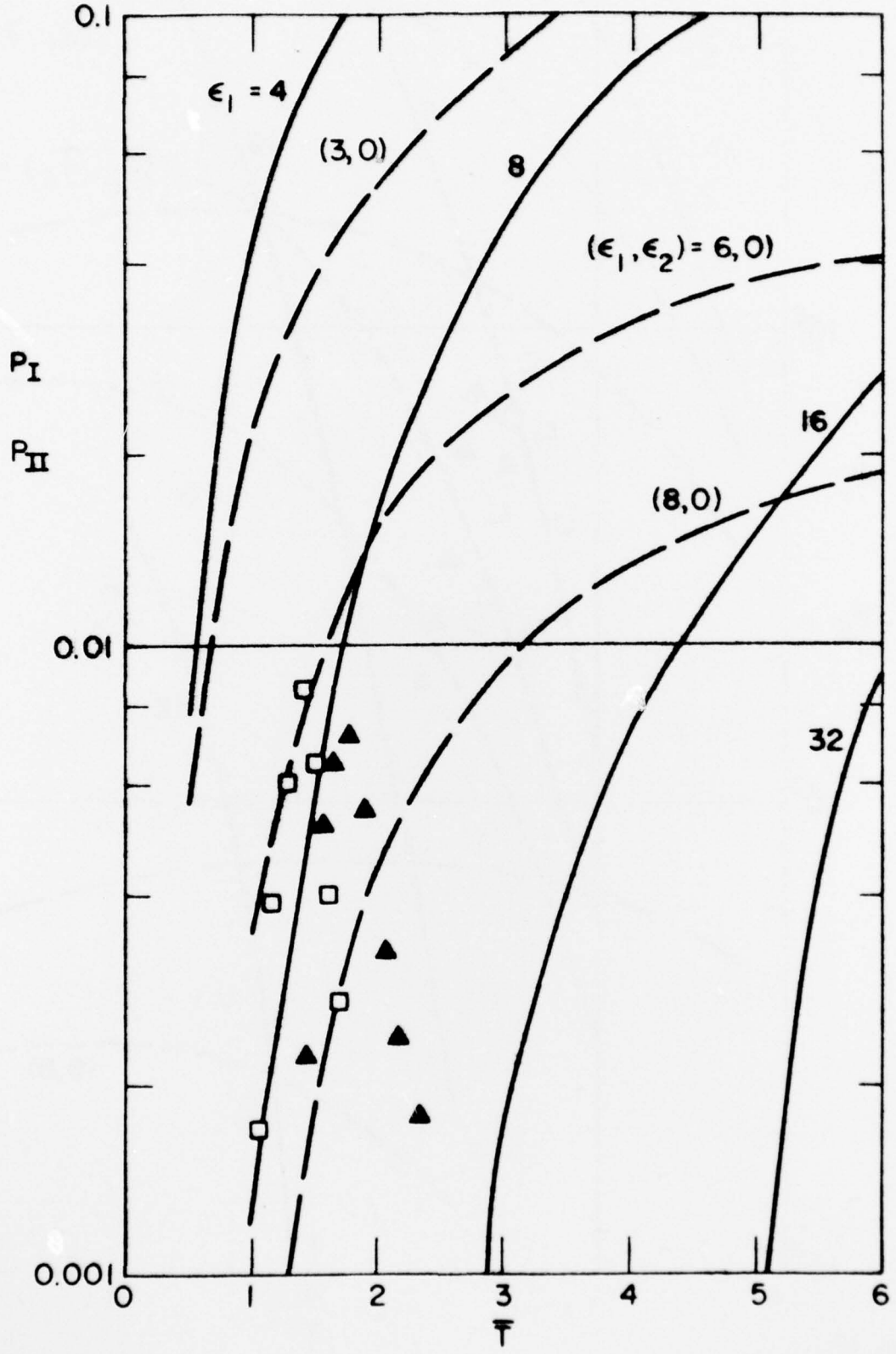

Fig. 9.

Collision Probabilities, $\mu = 8/3$, Experiment (O, ▲, □) for T_g = (300, 1475, 1875)° K.

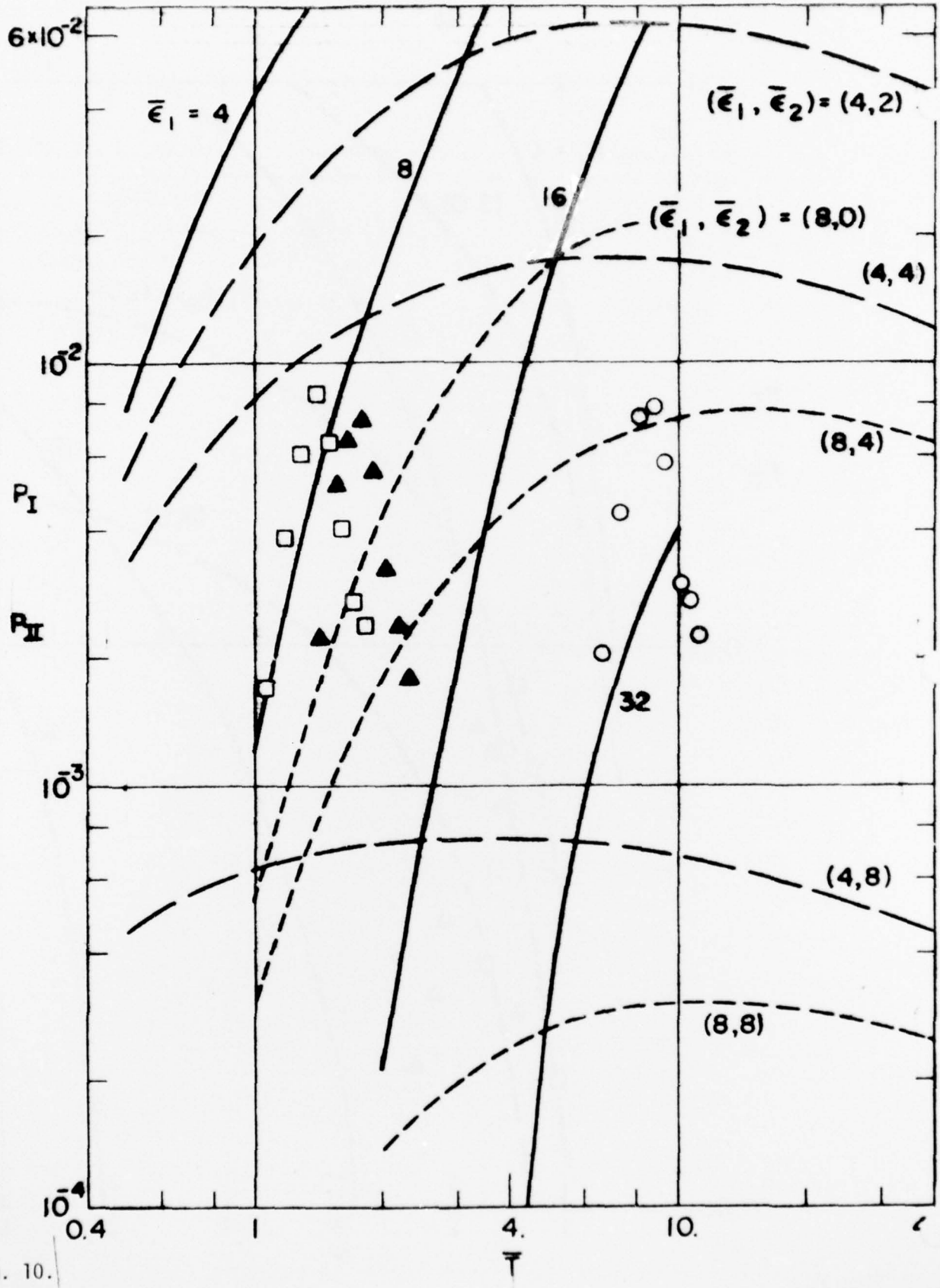

Fig. 10. Collision Probabilities, $\mu = 8/3$, Experiment (○,▲,□) for T_g = (300, 1475, 1875)° K.

REFERENCES

1. Allendorf, H.D. and Rosner, D.E., "Primary Products in the Attack of Graphite by Atomic Oxygen and Diatomic Oxygen Above 1100°K," Carbon, 7, p. 515, 1969.

2. Olander, D.R., Sickhaus, W., Jones, R. and Schwarz, J.A., "Reactions of Modulated Molecular Beams with Pyrolytic Graphite. I. Oxidation of the Basal Plane," J. Chem. Phys., 57, p. 408, 1972.

3. Shih, W.C.L., "Molecular Beam Studies of Graphite Oxidation," MIT Ph.D. Thesis, 1973.

4. Liu, G.N.-K., "High Temperature Oxidation of Graphite by a Dissociated Oxygen Beam," MIT Ph.D. Thesis, 1973.

5. Balooch, M., Cardillo, M.J., Miller, D.R. and Stickney,R.E., "Molecular Beam Study of the Apparent Activation Barrier Associated with Adsorption and Desorption of Hydrogen on Copper," Surface Science, 46, 2, p. 358, 1974.

6. Cardillo, M.J., Balooch, M. and Stickney, R.E., "Detailed Balancing and Quasiequilibrium in the Adsorption of Hydrogen on Copper," Surface Science, 50, 2. p. 263, 1975.

7. Van Willigen, W., "Angular Distribution of Hydrogen Molecules Desorbed from Metal Surfaces," Phys. Letters, 28A, 2, p. 80, 1968.

8. Palmer, R.L. and Smith, J.N., Jr., "Molecular Beam Study of CO Oxidation on a (111) Platinum Surface," J. Chem. Phys., 60, 4, p. 1453, 1974.

9. Dabiri, A.E., Lee, T.J. and Stickney, R.E., "Spatial and Speed Distribution of H_2 and O_2 Desorbed from a Polycrystalline Nickel Surface," Surface Science, 26, p. 522, 1971.

10. Logan, R.M. and Stickney, R.E., "Simple Classical Model for the Scattering of Gas Atoms from a Solid Surface," J. Chem. Phys., 44, 1, p. 195, 1966.

11. Goodman, F.O., "On the Theory of Accommodation Coefficients- IV. Simple Distribution Function Theory of Gas-Solid Interaction Systems," J. Phys. Chem. Solids, 26, p. 85, 1965.

12. Chapman, S. and Cowling, T.G., "The Mathematical Theory of Non-Uniform Gases," Cambridge University Press, 1953.

13. Grobner, W. and Hofreiter, N., "Integraltafel, Unbestimmte Integrale," Springer Verlag, Vienna, 1961.

14. Marsh, H., O'Hair, T.E. and Wynne-Jones, W.F.K., "Oxidation of Carbons and Graphite by Atomic Oxygen Kinetic Studies," Trans. Faraday Soc., 61, p. 274, 1965.

15. Thomas, J.M., "Reactivity of Carbon: Some Current Problems and Trends," Carbon, 8, p. 413, 1970.

16. Doak, R.B., "Activiation Studies in the Oxidation of Graphite," MIT S.M. Thesis, 1975.

UNCLASSIFIED

SECURITY CLASSIFICATION OF THIS PAGE (When Data Entered)

REPORT DOCUMENTATION PAGE	READ INSTRUCTIONS BEFORE COMPLETING FORM
1. REPORT NUMBER: AFOSR-TR-77-0102	2. GOVT ACCESSION NO.
	3. RECIPIENT'S CATALOG NUMBER: Technical rept.
4. TITLE (and Subtitle): REACTION PROBABILITIES IMPLIED BY MULTIPLE GAS-SURFACE INTERACTIONS.	5. TYPE OF REPORT & PERIOD COVERED: INTERIM
	6. PERFORMING ORG. REPORT NUMBER: Tech Rpt 76-1
7. AUTHOR(s): J. R. WILLIAMS, J. R. BARON	8. CONTRACT OR GRANT NUMBER(s): F44620-75-C-0040
9. PERFORMING ORGANIZATION NAME AND ADDRESS: MASSACHUSETTS INSITITUE OF TECHNOLOGY, AERONAUTICS AND ASTRONAUTICS DEPARTMENT, CAMBRIDGE, MA 02139	10. PROGRAM ELEMENT, PROJECT, TASK AREA & WORK UNIT NUMBERS: 681307, 2307A3, 61102F; 68p.
11. CONTROLLING OFFICE NAME AND ADDRESS: AIR FORCE OFFICE OF SCIENTIFIC RESEARCH/NA, BLDG 410, BOLLING AIR FORCE BASE, D C 20332	12. REPORT DATE: Dec 76
	13. NUMBER OF PAGES: 68
14. MONITORING AGENCY NAME & ADDRESS (if different from Controlling Office): 76-1	15. SECURITY CLASS. (of this report): UNCLASSIFIED
16. 2307	15a. DECLASSIFICATION/DOWNGRADING SCHEDULE

16. DISTRIBUTION STATEMENT (of this Report)

Approved for public release; distribution unlimited.

17 A3

17. DISTRIBUTION STATEMENT (of the abstract entered in Block 20, if different from Report)

18. SUPPLEMENTARY NOTES

19. KEY WORDS (Continue on reverse side if necessary and identify by block number)

GAS SURFACE INTERACTION
REACTION PROBABILITY
GRAPHITE OXIDATION

20. ABSTRACT (Continue on reverse side if necessary and identify by block number)

The probabilities of single and two successive gas surface collisions satisfying minimum interaction energy cutoffs are considered in the hard cube model sense. Comparison is made with atomic and molecular oxygen reaction probabilities with graphite corresponding to specific mass ratio examples of 4/3 and 8/3. Comparable peak probabilities result for multiple interactions but of much reduced sharpness with temperature for only a two collision constraint. Realistic activation energies are implied from a match of the energy cutoff probability model to the portion of the experimental data incresing with surface temperature. The rapidly

DD FORM 1 JAN 73 1473 EDITION OF 1 NOV 65 IS OBSOLETE

140250

UNCLASSIFIED

SECURITY CLASSIFICATION OF THIS PAGE (When Data Entered)

decreasing reaction probabilities found experimentally at higher temperatures imply an appreciable increase in the required number of effective collisions.